

POLISH POLAR RESEARCH	22	2	89–128	2001
-----------------------	----	---	--------	------

Krzysztof P. KRAJEWSKI<sup>1</sup>, Bożena ŁĄCKA, Michał KUŹNIARSKI, Ryszard ORŁOWSKI  
and Andrzej PREJBISZ

Instytut Nauk Geologicznych  
Polska Akademia Nauk  
Twarda 51/55, 00-818 Warszawa, POLAND

<sup>1</sup> Corresponding author (e-mail address: [kpkraj@twarda.pan.pl](mailto:kpkraj@twarda.pan.pl))

## Diagenetic origin of carbonate in the Marhøgda Bed (Jurassic) in Spitsbergen, Svalbard

**ABSTRACT:** The Marhøgda Bed is a carbonate-dominated lithostratigraphic unit occurring locally at base of the Middle–Late Jurassic organic-rich sequence of the Agardhfjellet Formation in Spitsbergen, Svalbard. It has been interpreted to represent oolitic limestone facies deposited during an initial stage of Late Jurassic transgression. Petrographic, major element geochemical, and stable carbon and oxygen isotopic data presented in this paper indicate that this lithostratigraphic unit is not a depositional limestone, but a diagenetic cementstone band originated in organic-rich sediment containing glauconite pellets and phosphatic ooids and grains. Two episodes of carbonate diagenesis, including early precipitation of siderite and burial precipitation of ankerite, have contributed to the development of this cementstone. Extensive siderite precipitation occurred at sedimentary temperatures in nearsurface suboxic environment in which microbial reduction of ferric iron was the dominant diagenetic process. Precipitation of ankerite occurred at temperatures of about 80–100°C in burial diagenetic environment overwhelmed by thermal decarboxylation processes. Formation of ankerite was associated with advanced alteration of glauconite, dissolution of apatite, and precipitation of kaolinite.

**Key words:** Svalbard, Spitsbergen, Jurassic, Marhøgda Bed, early diagenesis, burial diagenesis, carbonate minerals, palaeotemperatures.

### Introduction

The Marhøgda Bed has been defined by Bäckstrom and Nagy (1985) to classify carbonate band 30–150 cm thick occurring above the Brentskardhaugen Bed in the Middle–Late Jurassic transgressive sequence in central Spitsbergen. It has been interpreted to be an original limestone facies (oolitic microsparitic limestone), though showing advanced post-depositional alteration and replacement, mostly by Fe-rich carbonates. Occurrence of oolitic limestone at the transgressive

transition from condensed clastic shelf facies with common phosphate mineralization (Brentskardhaugen Bed) to organic-rich fine-grained shelf facies (Agardhfjellet Formation) seems, however, to be quite unusual, and it was questioned in several papers (Kopik and Wierzbowski 1988, Krajewski 1989, 1992a, b; Dypvik *et al.* 1991a, b). Despite these publications, the Marhøgda Bed has been referred to as 'oolitic limestone' in the recently published *Lithostratigraphic Lexicon of Svalbard* (Dallmann 1999), an official release of the *Committee on the Stratigraphy of Svalbard (SKS)* providing formal lithostratigraphic scheme of the Mesozoic sedimentary sequence in Svalbard.

The aim of this paper is to demonstrate that the Marhøgda Bed is not a depositional limestone facies. Petrographic, major element geochemical, and stable carbon and oxygen isotopic data are presented to support entirely diagenetic origin of carbonate in this lithostratigraphic unit.

## Geological setting

The Jurassic sedimentary sequence in Spitsbergen, Svalbard (Figs 1, 2) embraces marginal to shallow marine clastic deposits (Wilhelmøya Subgroup embracing the Knorringfjellet and Smalegga formations) which terminate in a highly condensed phosphorite horizon (Brentskardhaugen Bed), and are overlain by organic-rich shale facies of the Agardhfjellet Formation (Mørk *et al.* 1999). The sequence developed as a result of abandonment of Late Triassic deltaic systems (De Geerdalen Formation) and introduction of starved marine depositional regime in Early Jurassic Svalbard seaway; the latter expanded in Late Jurassic to form a broad shelf with organic-rich fine-grained deposition (Mørk *et al.* 1982, Steel and Worsley 1984, Dypvik *et al.* 1991a, b, Harland 1997). The Brentskardhaugen Bed represents a long depositional history (Toarcian–Bathonian), with several transgressive events interrupted by regressive episodes that led to alternative formation, reworking, and redeposition of nodular phosphorite (Birkenmajer 1972, Wierzbowski *et al.* 1981a, b, Bäckstrom and Nagy 1985; Maher 1989, Krajewski 1990, 1992a, b). Equalization of depositional conditions began in Late Bathonian as a result of general drowning of the Svalbard shelf (Birkenmajer 1975, Birkenmajer and Pugaczewska 1975, Kopik and Wierzbowski 1988, Krajewski 1989, Dypvik *et al.* 1991a, b). Transition from the Brentskardhaugen Bed to the overlying shale sequence of the Agardhfjellet Formation is gradational and associated with development of peculiar mineral deposits and sedimentary structures reflecting intermittent hiatal conditions during the onset of the Middle–Late Jurassic drowning (Pčelina 1980, Dypvik *et al.* 1991a, b; Krajewski 1992a, b). These deposits and structures embrace local accumulations of glauconite pellets, phosphatic and ferruginous ooids, as well as stromatolites, oncoids, and mats of agglutinated foraminifera (Fig. 3). They either form discontinuous pavements on phosphorite conglomerate of the Brentskardhaugen Bed or occur



Fig. 1. Sketch map of the Svalbard archipelago showing studied locations of the Marhøgda Bed in Spitsbergen.

concentrated in the basal part of the Agardhfjellet shale. The stromatolites and oncoids are subtidal biosedimentary structures that developed as a result of microbial phosphate authigenesis at the sea bottom, foraminiferal encrustation, and trapping and binding of various detrital sediment grains (Krajewski 1992a). The ooids show

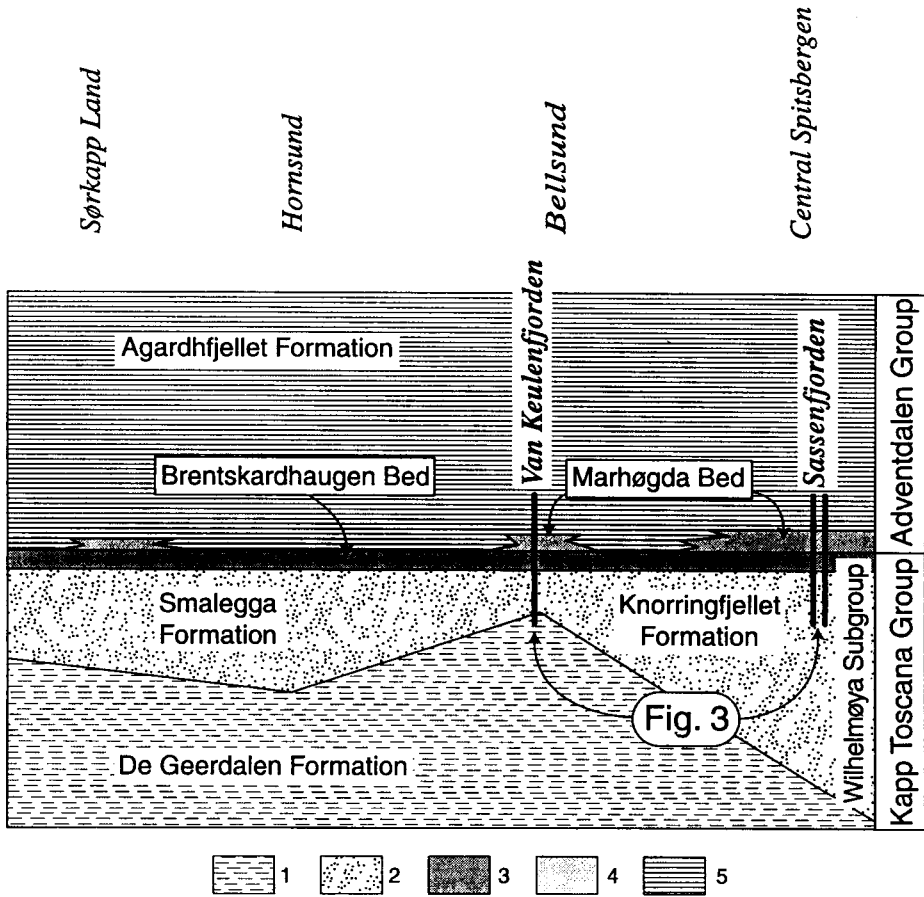


Fig. 2. Lithostratigraphic scheme of Late Triassic–Jurassic sedimentary sequence in Spitsbergen showing location of the studied sections of the Marhøgda Bed. Lithostratigraphic scheme after Mørk *et al.* (1999), simplified. 1 – deltaic facies; 2 – marginal to shallow marine starved clastic facies; 3 – condensed conglomeratic phosphorite-bearing horizon; 4 – transitional deposits (glauconite pellets, phosphatic ooids and grains, stromatolites, and oncoids in sandy to muddy sediment, variably cemented and/or replaced by diagenetic carbonate); 5 – grey to black organic-rich shelf shale with recurrent carbonate cementstone bands and concretions.

several stages of cortex growth separated by discontinuity surfaces and/or accreted silty material, suggesting stages of their development within fine-grained sediment and frequent winnowing.

Deposition of organic-rich facies of the Agardhfjellet Formation and diagenetic and burial decomposition of organic matter contained in it aided the formation of recurrent bands and concretionary horizons of carbonate cementstone in the shale sequence ((Dypvik 1978, 1985; Krajewski 1992a, Bausch *et al.* 1998). They consist of a complex mixture of iron, magnesium, and calcium carbonates occurring at various proportions with clay minerals and detrital sediment fractions,

though siderite is commonly the dominant component. Similar cementstone bands and concretions also occur in organic-rich fine-grained intervals of the Knorringfjellet Formation.

A cementstone band is locally present at base of the Agardhfjellet sequence, where it variably cements and replaces glauconitic-phosphatic deposits occurring above the Brentskardhaugen Bed (Fig. 3). This band is particularly well developed at the southern margin of Sassenfjorden where it has been classified into the Marhøgda Bed by Bäckstrom and Nagy (1985). It can also be seen in the Sassen-dalen outcrop belt, in the Festningen section in Isfjorden and at Agardhbukta in eastern Spitsbergen. At the southern margin of Sassenfjorden (Deltanaset, Konusdalen, Marhøgda, Wimanfjellet, Knorringfjellet, Botneheia), the band is pale grey to yellowish in colour and contains common carbonate- and kaolinite-replaced glauconite pellets and phosphatic ooids and grains, which makes that the rock might be mistaken for oolitic limestone deposit. The rock shows traces of sediment bioturbation and contains scattered chert pebbles as well as numerous carbonate-replaced belemnite rostra. No other macrofossils have been found in the Marhøgda Bed, though carbonate cementstones occurring higher up in the sequence yielded moulds of ammonites and bivalves (Kopik and Wierzbowski 1988). The Marhøgda Bed has a sharp lower boundary towards the underlying Brentskardhaugen Bed. Its upper boundary is gradational and consists in an upward decrease of the content of carbonate cement coupled with an increase of the content of clay minerals and fine detrital fractions (Fig. 3). The Bed is overlain by a sequence of grey bioturbated siltstone, sandy siltstone and shale of the Oppdalen Member (Krajewski 1989, Dypvik *et al.* 1991a, b; Mørk *et al.* 1999).

Diagenetic alteration of the transitional deposits above the Brentskardhaugen Bed is less pronounced in the Bellsund area, where phosphatic accumulations occurring at base of the Agardhfjellet Formation show mostly incipient stages of carbonate replacement (Krajewski 1992a). In the Ingebrigtsenbukta section in Van Keulenfjorden, the Marhøgda Bed consists of the lower part dominated by phosphatic/siliciclastic stromatolites and mats of agglutinated foraminifera directly covering the Brentskardhaugen phosphorite conglomerate, and the upper part composed of siltstone and fine-grained sandstone with common phosphatic ooids, nodules and clasts (Fig. 3). The content of sandy grains and phosphatic ooids decreases upwards, and the Bed passes gradually into black, organic-rich siltstone and laminated shale with recurrent cementstone bands (informal Ingebrigtsenbukta member of the Agardhfjellet Formation; Różycki 1959, Mørk *et al.* 1999).

In the Hornsund area, the transitional deposits are widely absent, and the Agardhfjellet shale directly overlies the Brentskardhaugen phosphorite conglomerate (Birkenmajer 1975, Krajewski 1992b). In Sørkapp Land, transitional deposits attributed to the Marhøgda Bed occur locally in the Karentoppen area (Krajewski 1992b). They are represented by phosphatic and ferruginous oncoids and ooids cemented and replaced to a various extent by diagenetic carbonate.

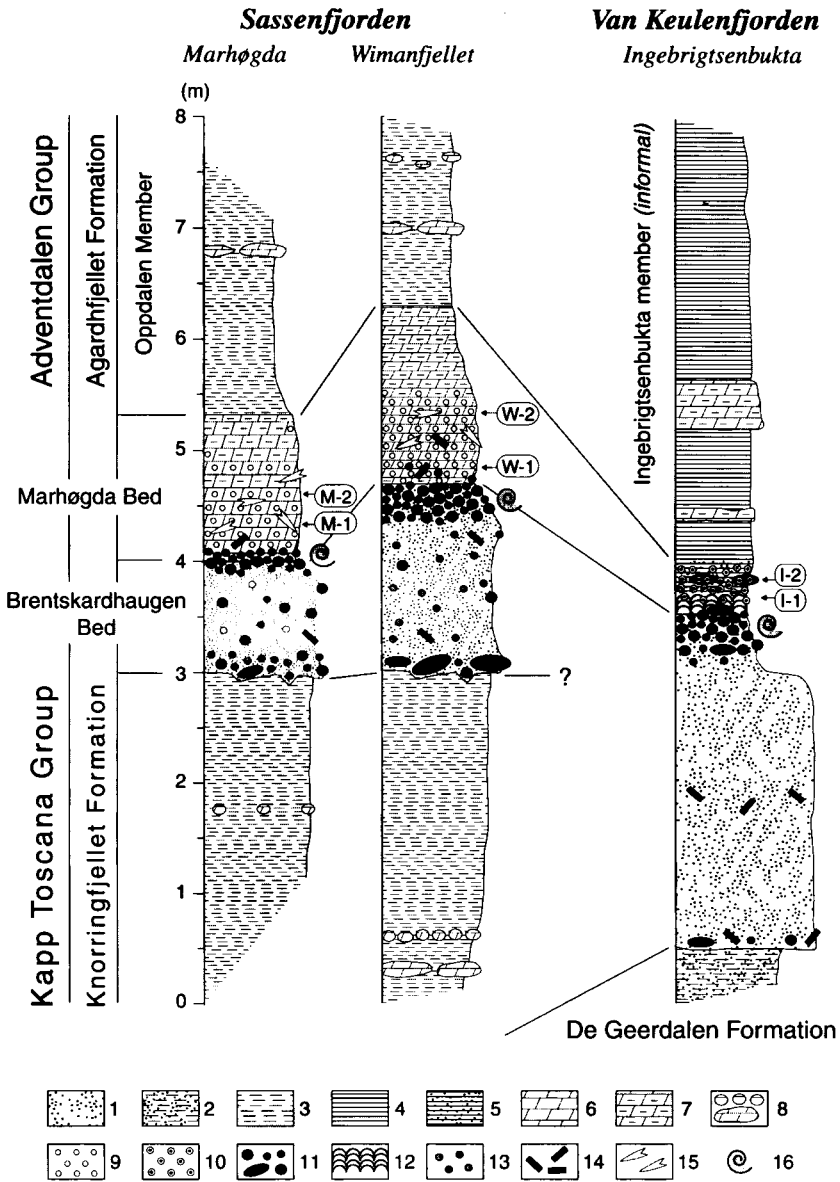


Fig. 3. Sections of the Brentskardhaugen and Marhøgda beds at Marhøgda, Wimanfjellet (Sassenfjorden) and Ingebrigtsenbukta (Van Keulenfjorden) in Spitsbergen. M-1, M-2, W-1, W-2, I-1, and I-2 are samples analyzed for the carbon and oxygen isotopic composition of carbonate minerals. 1 – medium- to coarse-grained sandstone and conglomerate; 2 – sandy shale and shaly sandstone; 3 – grey shale, mudstone and siltstone; 4 – black shale, mudstone and siltstone; 5 – black sandy shale and mudstone; 6 – carbonate cementstone bands; 7 – clay-rich carbonate cementstone bands; 8 – concretionary carbonate cementstone; 9 – carbonate- and kaolinite-replaced pellets, ooids and grains; 10 – phosphatic ooids (partly replaced by diagenetic carbonate); 11 – phosphate nodules and pebbles; 12 – phosphatic stromatolite (partly replaced by diagenetic carbonate); 13 – quartz and chert pebbles; 14 – wood fragments (commonly phosphatized); 15 – belemnite rostra (replaced by diagenetic carbonate); 16 – fossiliferous horizons.

## Materials and methods

The present study is based on three sections of the Marhøgda Bed, i.e. the Marhøgda and Wimanfjellet sections at the southern margin of Sassenfjorden, and the Ingebrigtsenbukta section at the southern margin of Van Keulenfjorden (Fig. 3). These locations provide an insight into advanced and incipient stages of diagenetic sediment alteration at base of the Agardhfjellet Formation, respectively.

18 polished thin sections of the Marhøgda Bed were analyzed using standard petrographic methods, including transmitted (TLM) and reflected light microscopy (RLM), back-scattered electron imaging (BSE) and energy-dispersive X-ray spectroscopy (EDS). BSE images were obtained using a CAMECA SX 100 microprobe with back-scattered electron detector and a JEOL JSM-840A microscope, both operating at 15 kV acceleration voltage. Quantitative EDS analyses of carbonate minerals were obtained using a JEOL JSM-840A equipped with a LINK ANALYTICAL spectrometer AN 1000/85S. Operating conditions were a 15 kV acceleration voltage, 1 to 5  $\mu\text{m}$  beam diameter, and 100 s counting time. Detection limits of the analyzed elements (Ca, Mg, Fe, and Mn) were better than 0.1 wt %. EDS data were recalculated as cation mole fractions to facilitate comparisons among samples.

Mineralogic composition of six samples (M-1, M-2, W-1, W-2, I-1, and I-2) was analyzed by means of X-ray diffraction. The detailed location of these samples is shown in Fig. 3. Carbonate-replaced pellets, ooids, and grains were hand picked from crushed samples in the Marhøgda and Wimanfjellet sections and analyzed separately. Samples were ground to < 63  $\mu\text{m}$  fraction using an agate mortar and pestle. Diffraction patterns were recorded on a SIGMA 2070 diffractometer using a curved position sensitive detector in the range 2–120° 2 $\theta$  with CoK $\alpha$  radiation and 20 h analysis time. DIFFRACTIONEL software v. 03/93 was used to process the obtained data.

The same samples and size fraction were analyzed for the carbon and oxygen isotopic composition of carbonate minerals. Crushed rock fragments were hand picked under a binocular microscope to provide material with maximum content of carbonate minerals. CO<sub>2</sub> for isotopic analyses was produced from samples by reaction with anhydrous phosphoric acid ( $d = 1.90 \text{ g cm}^{-3}$ ) at 25° C. In an attempt to discriminate between end members of carbonate mixtures, the samples were treated by a progressive leach procedure, with a time sequence of CO<sub>2</sub> collecting. CO<sub>2</sub> from siderite-ankerite dominated samples (Marhøgda, Wimanfjellet) was collected after 20, 120, and 168 hours of reaction. CO<sub>2</sub> collected after 20 and 120 h represents mostly ankerite, whereas the one collected after 168 h represents siderite, though the reaction of siderite with phosphoric acid was not yet completed (about 30% of siderite was dissolved). Duplicated samples were treated for 4 h at 100°C after 120 h treatment at 25°C. CO<sub>2</sub> was collected after 124 h, with a portion of gas discarded after 120 h. Application of this procedure has led to complete dis-

solution of siderite, though sample treatment with phosphoric acid at 100°C might affect decomposition of organic compounds, thus leading to contamination of sideritic CO<sub>2</sub> with organic CO<sub>2</sub>. CO<sub>2</sub> derived from ankerite-apatite dominated samples (Ingebrigtsenbukta) was collected after 20, 48 and 96 hours of reaction at 25°C. It represents a mixture of ankeritic CO<sub>2</sub> and CO<sub>2</sub> derived from lattice-bound CO<sub>3</sub><sup>2-</sup> in carbonate fluorapatite (CFA). The calculated content of CO<sub>2</sub> in the CFA crystal lattice (using the obtained XRD data and the equations of Gulbrandsen 1970 and Schuffert *et al.* 1990) is approx. 2.6%, suggesting that contribution of CFA-derived CO<sub>2</sub> in the collected gas is negligible. Oxygen isotope fractionation factors  $\alpha = 1.01169$ ,  $\alpha = 1.01098$  and  $\alpha = 1.00881$  were used for siderite and ankerite (25°C) and siderite (100°C), respectively (Becker and Clayton 1976, Rosenbaum and Sheppard 1986).

Isotopic <sup>13</sup>C/<sup>12</sup>C and <sup>18</sup>O/<sup>16</sup>O ratios were determined using a FINNIGAN MAT DELTA<sup>PLUS</sup> spectrometer working in dual inlet mode with universal triple collector. The  $\delta$  values were calculated relative to isotopic ratios of the international standard NBS 19. The results are expressed as  $\delta^{13}\text{C}$  and  $\delta^{18}\text{O}$  notations with respect to VPDB (Vienna Peedee Belemnite). Analytical reproducibility in laboratory was better than  $\pm 0.05\text{‰}$  and  $\pm 0.1\text{‰}$  for  $\delta^{13}\text{C}$  and  $\delta^{18}\text{O}$ , respectively.

## Results

### Petrography

**Sassenfjorden.** — The Marhøgda Bed at the southern margin of Sassenfjorden consists of siderite-dominated matrix containing abundant carbonate/kaolinite-replaced moulds of glauconite pellets and phosphatic ooids and grains (Figs 4A, 5), as well as various detrital sediment grains (mostly quartz and chert) and biogenic debris (diagenetically altered fragments of belemnite skeletons, fish tooth fragments, and arenaceous forams). XRD data show that the Bed is composed of siderite, ankerite, kaolinite, quartz, and glauconite-illite in order of abundance (Fig. 6). Concentrated pellets, ooids and grains show different order of mineral abundance, with ankerite being the dominant component (Fig. 7). Carbonate fluorapatite (CFA) becomes X-ray detected in the concentrated fraction. No X-ray detectable calcite has been revealed in the analyzed samples. There is also no evidence of the presence of chamosite, as it was postulated earlier by Dypvik *et al.* (1991a, b).

The matrix is composed of a sideritic mosaic containing changing amounts of clay minerals (illite prevailing over kaolinite), fine quartz detritus, and CFA. Siderite occurs principally as microcrystalline rhombs ranging in size from 3 to 15  $\mu\text{m}$ . Detailed mineral composition of the matrix changes on a microscale, reflecting changing intensity of diagenetic siderite formation (Fig. 8). At places, the matrix contains irregular seams (20–200  $\mu\text{m}$ ) composed of clay minerals embedding fine CFA particles. The matrix closely embeds diagenetically altered pellets, ooids and grains, though the sideritic groundmass usually imprints their external surfaces

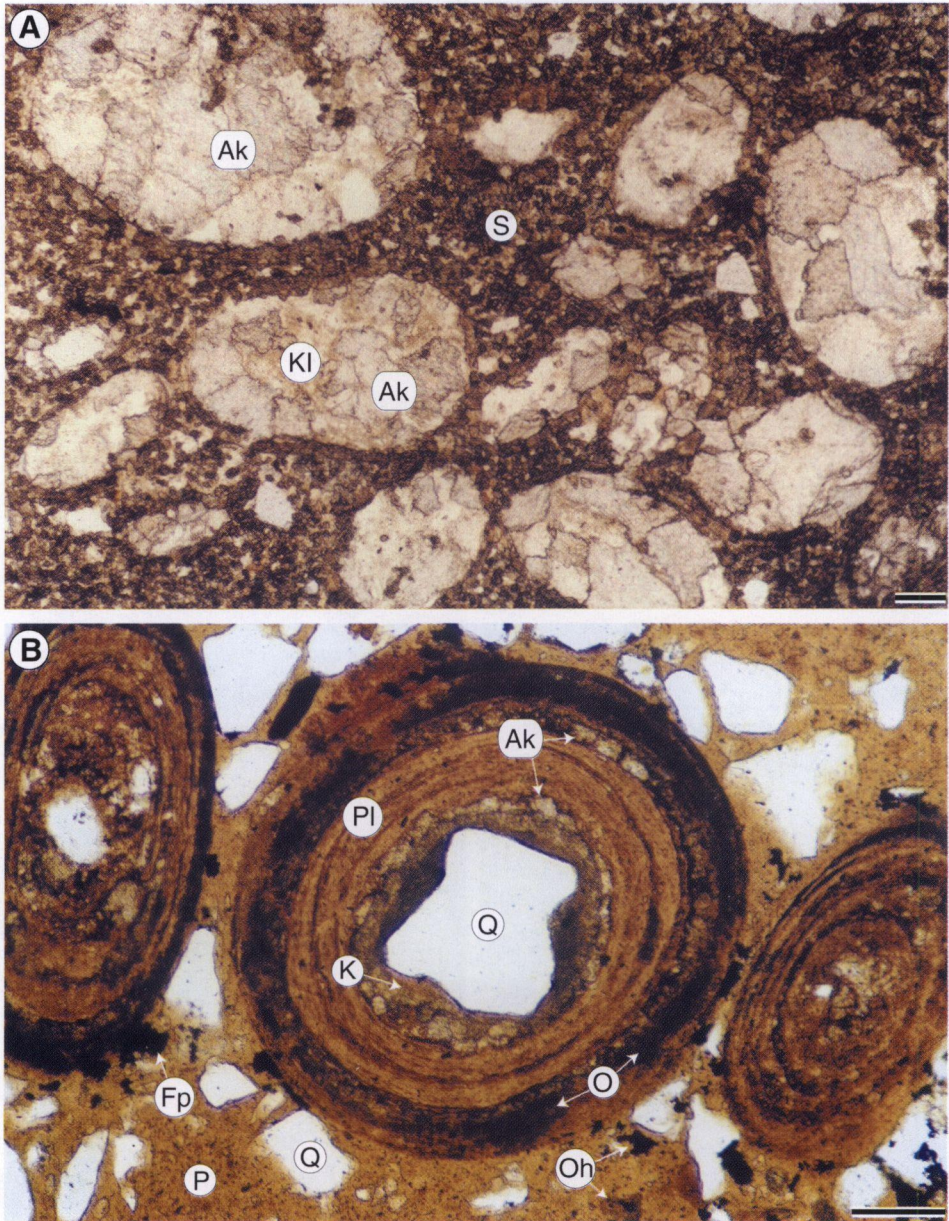


Fig. 4. Petrographic development of the Marhøgda Bed at the southern margins of Sassenfjorden (A) and Van Keulenfjorden (B). A. Early diagenetic microsparitic siderite (S) forming matrix of the Marhøgda Bed at Marhøgda contains common rounded objects replaced by late diagenetic ankerite crystals (Ak) and kaolinite-illite aggregates (KI). Rare remnants of the original sediment composition (not visible on the photo) suggest that the objects were glauconite pellets and phosphatic ooids and grains prior to their diagenetic alteration. B. Phosphatic ooids composed of laminated, submicroscopic CFA (Pl) in silty/sandy phosphatic nodule in the Marhøgda Bed at Ingebrigtsenbukta. The ooids are commonly developed around quartz grains (Q) and contain lamina variably enriched in organic matter (O). They show incipient stages of replacement by diagenetic ankerite (Ak) and kaolinite (K). The nodular matrix consists of quartz grains (Q) cemented by submicroscopic CFA (P). It contains framboidal pyrite (Fp) and pyritized herbaceous organic remains (Oh). A, B – TLM photomicrographs, normal light; scale bars = 100  $\mu$ m.

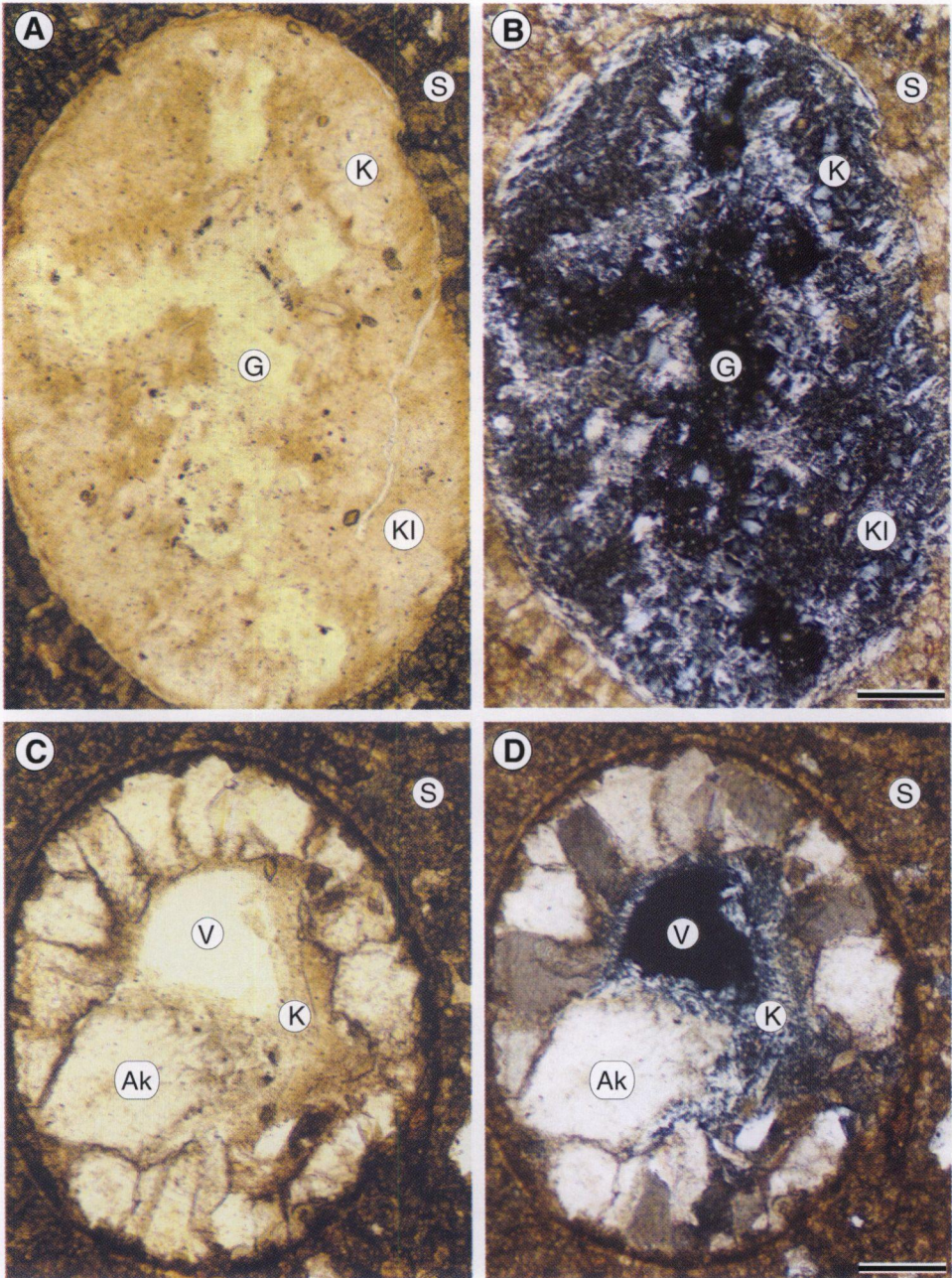


Fig. 5. Diagenetic alteration of glauconite pellets and phosphatic ooids in the Marhøgda Bed at the southern margin of Sassenfjorden. **A, B.** Glauconite pellet occurring in sideritic matrix (*S*) shows advanced alteration to kaolinite and illite. Remnants of the original glauconitic fabric (*G*) are yellowish to pale green, suggesting significant removal of iron from the mineral lattice. The replacement fabric consists of a mixture of kaolinite and illite (*KI*), and encapsulates vermicular aggregates of pure kaolinite (*K*). **C, D.** Mould after dissolution of phosphatic ooid in sideritic matrix shows complex infilling by diagenetic minerals. Subhedral to anhedral ankerite crystals (*Ak*) grew from the external mould surface inwards forming bulk of the replacement structure. They are covered by irregular concentric zone made up of kaolinite (*K*). The mould centre remains as void (*V*). *A, C* – TLM photomicrographs, normal light; *B, D* – crossed nicols; scale bars = 100  $\mu\text{m}$ .

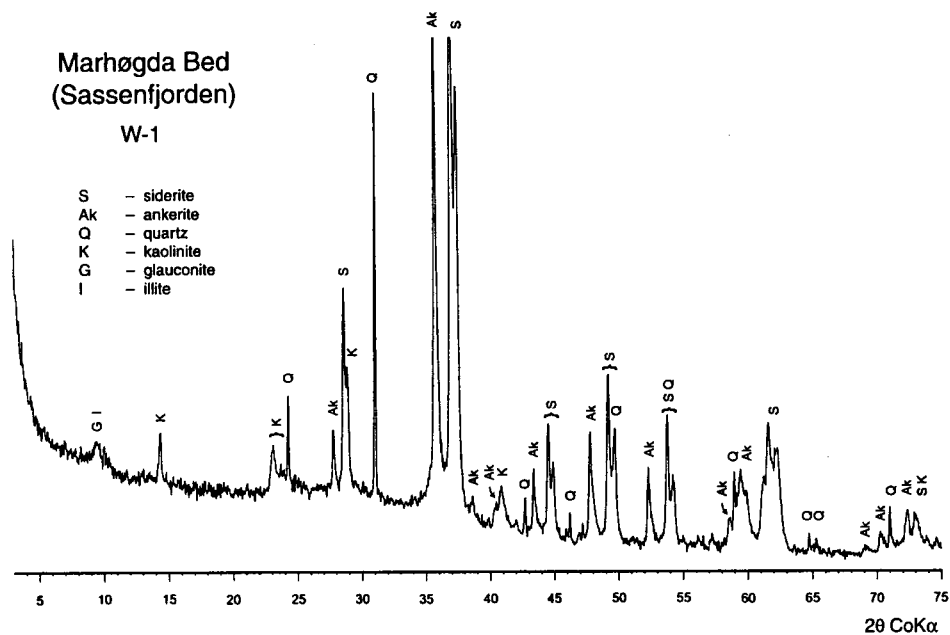


Fig. 6. Mineral composition of the Marhøgda Bed at the southern margin of Sassenfjorden (I). X-ray diffraction pattern of sample W-1 in the Wimanfjellet section.

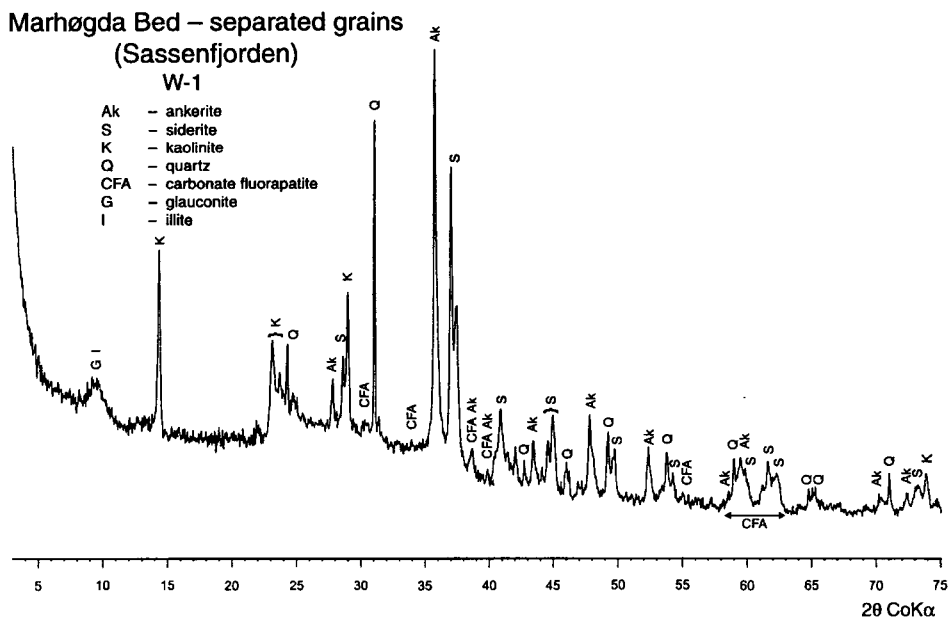


Fig. 7. Mineral composition of the Marhøgda Bed at the southern margin of Sassenfjorden (II). X-ray diffraction pattern of separated pellets, ooids and grains from sample W-1 in the Wimanfjellet section.

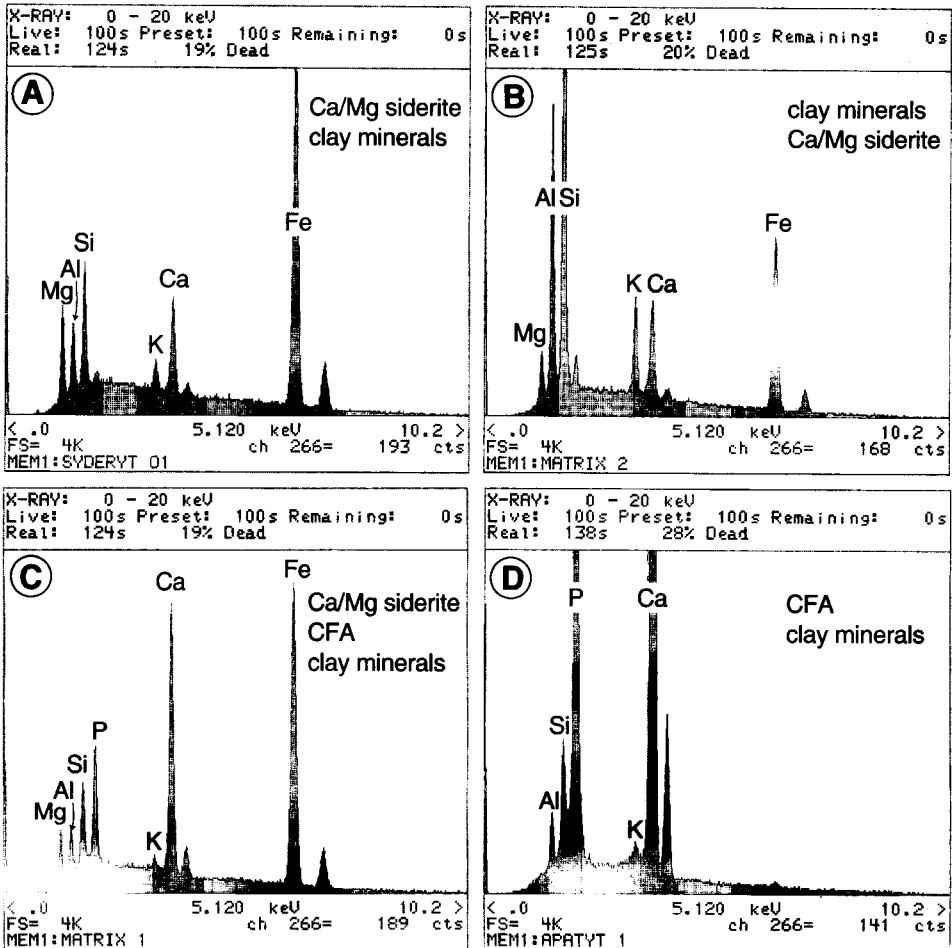


Fig. 8. Compositional variations of matrix of the Marhrgda Bed at the southern margin of Sassenfjorden. EDS spectra and inferred mineral composition of matrix in sample M-2 in the Marhøgda section.

without advanced corrosion or diagenetic modification. In many cases, however, there were observed compact sideritic rims (5–20  $\mu\text{m}$  thick) around the grains showing uneven internal boundaries, which suggest partial penetration of siderite into the original mineral fabric of the grains before their diagenetic replacement.

Pellets, ooids and grains (200  $\mu\text{m}$  – 3 mm, rarely up to 10 mm in size) are variably replaced by subhedral to anhedral ankerite crystals and clay aggregates dominated by kaolinite (Figs 4A, 5). Ankerite crystals (50–400  $\mu\text{m}$ ) grew from the external pellet/ooid boundaries inwards or from scattered internal nucleation sites, consequently replacing the original mineral material. They are also noted to infill mouldic pores developed as a result of diagenetic dissolution of the grains. Kaolinite aggregates occur either in the form of irregular replacement zones in the grains or as concentric zones that fringe internal boundaries of the ankeritic fabric.

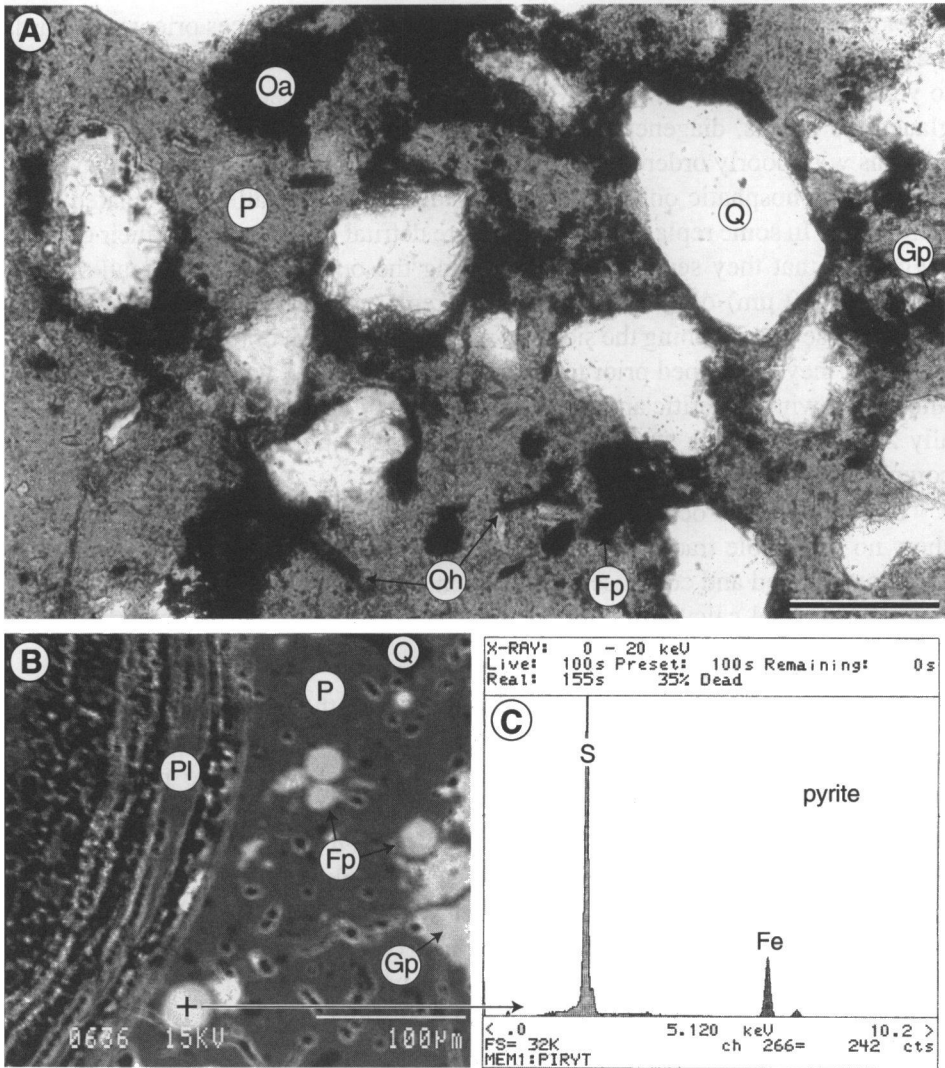


Fig. 9. Pyrite and organic matter in the Marhøgda Bed at the southern margin of Van Keulenfjorden. **A.** Phosphatic silty sandstone consists of quartz grains (*Q*) cemented by submicroscopic CFA (*P*). The matrix contains abundant amorphous (*Oa*) and herbaceous organic matter (*Oh*), and framboidal (*Fp*) and microgranular pyrite (*Gp*). TLM photomicrograph, normal light; scale bar = 100 µm. **B.** BSE image showing framboidal (*Fp*) and microgranular pyrite (*Gp*) in phosphatic matrix (*P*) containing silt-size quartz grains (*Q*). A part of phosphatic ooid visible in the photo is composed of laminated, ultramicrocrystalline CFA (*Pl*). **C.** EDS spectrum of framboidal pyrite shown in *B*.

Commonly observed replacement structure consists of an external pellet/ooid part composed of ankerite crystals, with the central part occupied by aggregates of clay minerals (kaolinite prevailing over illite) and ankerite. Rarely observed, incipient stages of the replacement embrace glauconite pellets and phosphatic ooids show-

ing external rims of ankerite crystals with crystallographic faces oriented towards the pellet/ooid centres. Remnants of the original glauconite usually are pale green to yellowish in colour under TLM, suggesting its advanced alteration to illite. In glauconite pellets, diagenetic kaolinite usually occurs in the form of fine intergrowths with poorly ordered illite. Only in a few cases well-preserved glauconite pellets and phosphatic ooids composed of ultramicrocrystalline, laminated CFA were noted. In some replaced ooids, there are detrital quartz grains in their centres, suggesting that they served as nuclei during the ooid formation. Small siderite rhombs (5–20  $\mu\text{m}$ ) occur scattered in the replaced grains. They resemble very closely those ones forming the sideritic matrix. The nature of their boundaries suggests that they developed prior to ankerite formation, and were then incorporated into the growing ankeritic and/or kaolinitic fabric. Large ankerite crystals are usually zoned, suggesting stages of their growth associated with varying chemical composition of fluids from which they precipitated.

Belemnite rostra occurring in the Marhøgda Bed are replaced by ankerite and show no detectable traces of the original calcite. The replacement structures are commonly zoned and composed of a sequence of cement generations, suggesting stages of skeletal calcite dissolution and precipitation of diagenetic carbonate in the mouldic pore space.

**Van Keulenfjorden.** — The Marhøgda Bed at the southern margin of Van Keulenfjorden consists of siltstone and silty sandstone containing common phosphatic ooids, grains, and nodules (Fig. 4B). Detrital grains are mostly quartz (25–150  $\mu\text{m}$ ), with a negligible admixture of feldspar, though quartz and chert pebbles up to 30 mm in size occur scattered in the sediment. The matrix contains framboidal and microgranular pyrite as well as variably pyritized amorphous and herbaceous organic matter. Nodules and clasts (up to several centimetres in size) are composed of silty to sandy phosphatic matrix containing abundant phosphatic ooids. Framboidal and microgranular pyrite, as well as organic matter also occur in phosphatic nodular matrices (Fig. 9). XRD data show that the phosphate is represented by a well-crystalline CFA (Fig. 10).

Phosphatic ooids range in size from 300  $\mu\text{m}$  up to a few millimetres. The ooids are frequently developed around quartz grains, and made up of ultramicroscopic, laminated CFA (Fig. 4B). Lamination is accentuated by thin films enriched in organic inclusions. Complexity of the cortex structure increases with the increasing ooid size. Large ooids usually show many generations of cortex growth separated by discontinuity surfaces and seams of accreted fine detrital material. There also occur clasts composed of a few phosphatic ooids cemented by phosphatic matrix, and showing abrasional external boundaries. Clasts of phosphatic siltstone and compact submicroscopic CFA, as well as glauconite pellets and fish debris occur as subordinate components.

Phosphatic ooids and grains show various stages of diagenetic replacement by ankerite and kaolinite (Figs 11, 12). The two diagenetic minerals are closely asso-

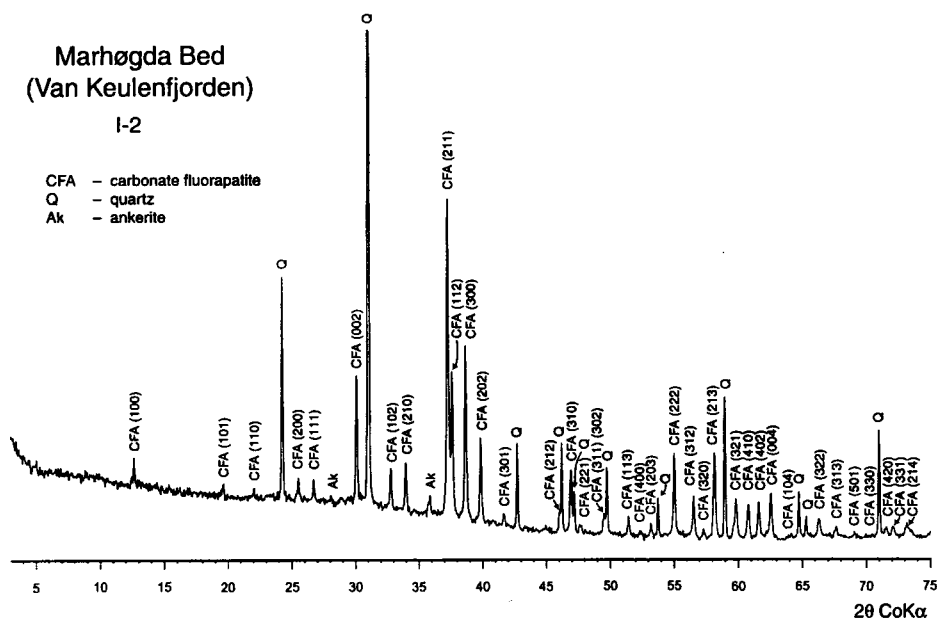


Fig. 10. Mineral composition of the Marhøgda Bed at the southern margin of Van Keulenfjorden. X-ray diffraction pattern of sample I-2 in the Ingebrigtsenbukta section.

ciated, commonly forming a mixed carbonate-kaolinite fabric that contains remnants of the original laminated CFA. However, there are noted ooids and grains, in which either ankerite or kaolinite dominates the replacement structure. Replacement structures in ooids occurring in the silty matrix are similar to the ones observed in the Marhøgda Bed at Sassenfjorden. Ooids occurring in silty to sandy phosphatic nodules show mostly incipient replacement structures.

There are two different morphologic types of ankerite in the analyzed material: (1) anhedral to subhedral crystals (30–400  $\mu\text{m}$ ) forming compact to sieve replacement structures or occurring scattered in ooid cortexes (Fig. 11A); and (2) subhedral to acicular crystals (5–100  $\mu\text{m}$ ) forming concentric replacement zones and intergrowths with kaolinite aggregates in ooid cortexes (Fig. 11B). The type (1) crystals show indistinct zonation under TLM and in BSE images. Paragenetic relationship between the ankerite types is difficult to reveal because they are seldom observed to occur as intergrowing fabric. Rare examples suggest that type (1) is slightly earlier than type (2).

### Major element geochemistry

The results of microprobe compositional analyses of carbonate minerals in the Marhøgda Bed are listed in Tables 1–5.

The matrix-forming siderite of the Marhøgda Bed at Sassenfjorden is enriched in Ca and Mg, and has very low Mn content (up to 0.6 mol %). The siderite shows

Table 1

Chemical composition of siderite in the Marhøgda Bed at the southern margin of Sassenfjorden

Sassenfjorden – chemical composition of siderite					
Location	Analysis	CaCO <sub>3</sub>	MgCO <sub>3</sub>	FeCO <sub>3</sub>	MnCO <sub>3</sub>
		mol %			
Marhøgda	1	14.88	13.14	71.98	–
	2	14.20	12.36	73.44	–
	3	10.13	12.97	76.76	0.13
	4	14.40	12.99	72.61	–
	5	5.54	15.24	78.98	0.25
	6	8.11	14.85	77.05	–
	7	15.45	14.82	69.72	–
	8	17.28	10.44	72.27	–
	9	14.11	12.10	73.79	–
	10	7.78	15.44	76.78	–
Wimanfjellet	11	12.75	12.72	74.35	0.18
	12	13.79	13.63	72.01	0.57
	13	13.70	18.08	68.22	–
	14	14.08	12.04	73.89	–
	15	7.09	11.52	81.19	0.20
	16	9.09	14.37	76.21	0.33
	17	7.41	22.66	69.71	0.22
	18	14.96	14.21	70.83	–
	19	4.41	23.42	72.11	0.06
	20	13.18	11.75	75.07	–

Table 2

Chemical composition of ankerite in the Marhøgda Bed at the southern margin of Sassenfjorden

Sassenfjorden – chemical composition of ankerite					
Location	Analysis	CaCO <sub>3</sub>	MgCO <sub>3</sub>	FeCO <sub>3</sub>	MnCO <sub>3</sub>
		mol %			
Marhøgda	1	59.32	28.04	12.47	0.17
	2	58.65	27.90	13.35	0.10
	3	59.78	26.04	14.18	–
	4	59.15	28.10	12.68	0.07
	5	59.40	28.08	12.40	0.13
	6	58.83	27.18	13.84	0.16
	7	58.48	28.95	12.49	0.08
	8	59.15	28.28	12.47	0.10
	9	59.65	27.43	12.91	–
	10	59.34	28.48	12.12	0.06
Wimanfjellet	11	59.26	24.76	15.98	–
	12	58.55	29.84	11.46	0.15
	13	58.88	26.96	13.88	0.28
	14	58.98	28.51	12.48	0.03
	15	60.09	24.81	14.85	0.25
	16	59.02	29.30	11.68	–
	17	59.37	27.82	12.79	0.02
	18	59.04	29.86	11.10	–
	19	58.32	30.19	11.42	0.07
	20	58.72	27.74	13.54	–

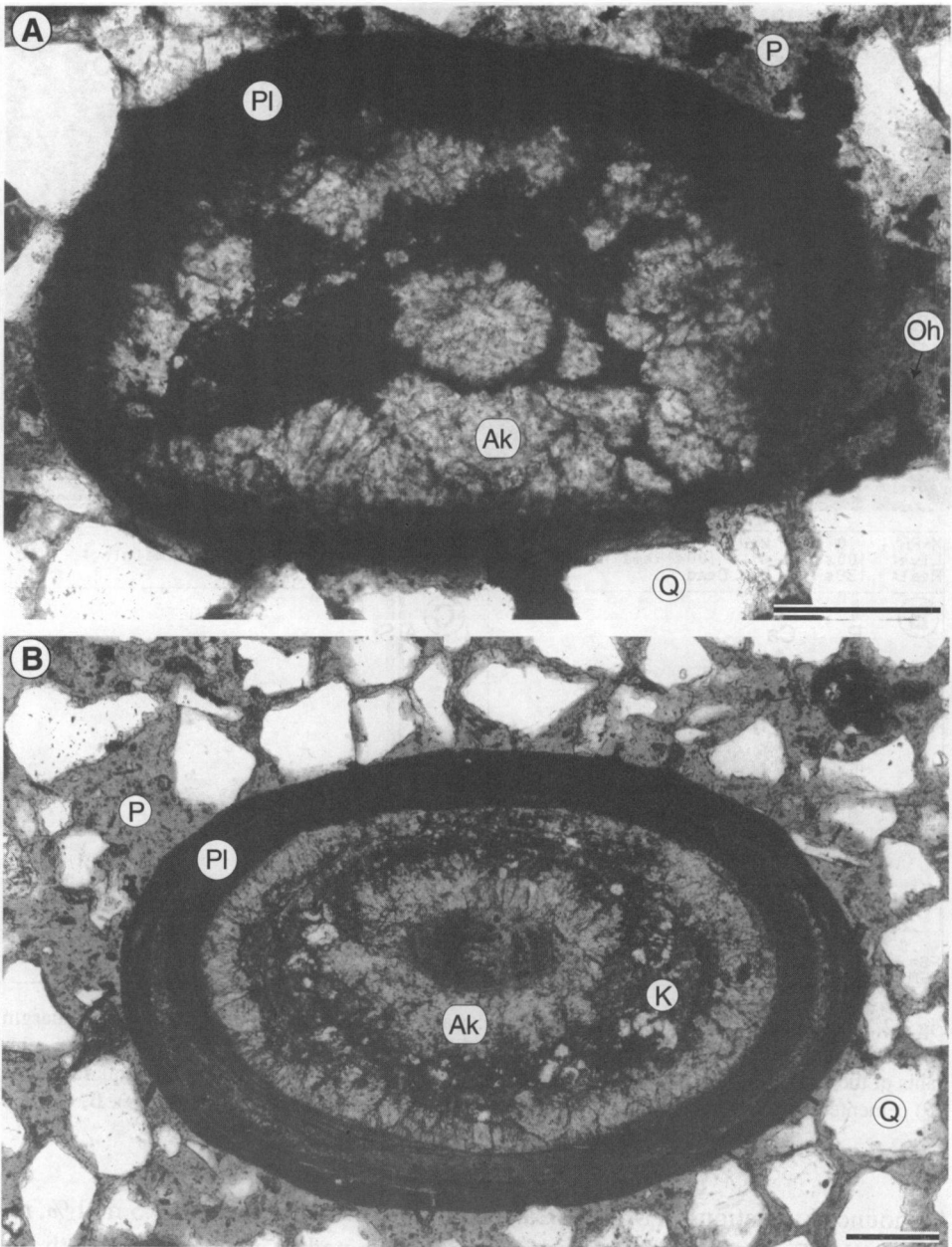


Fig. 11. Morphologic types of ankerite replacing phosphate ooids in the Marhøgda Bed at the southern margin of Van Keulenfjorden. **A.** Subhedral ankerite crystals (*Ak*) forming irregular replacement zone in ooid composed of laminated, ultramicrocrystalline CFA (*Pl*). **B.** Concentric replacement zones composed of acicular to subhedral ankerite (*Ak*) separated by a zone composed of diagenetic kaolinite (*K*) in ooid composed of laminated, ultramicrocrystalline CFA (*Pl*). The ooids occur in phosphatic silty sandstone composed of quartz grains (*Q*) cemented by ultramicrocrystalline CFA (*P*). Herbaceous organic matter (*Oh*) occurs in the matrix. *A, B* – TLM photomicrographs, normal light; scale bars = 100  $\mu$ m.

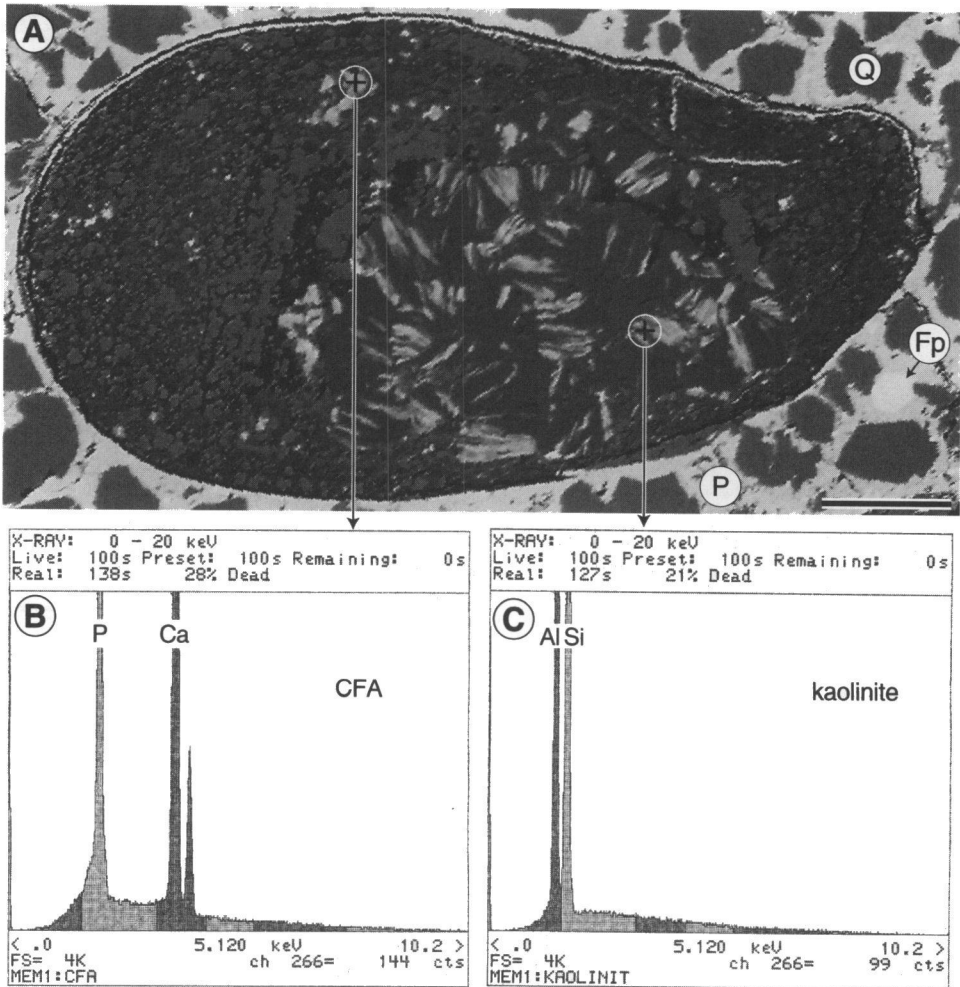


Fig. 12. Diagenetic kaolinite replacing phosphatic grain in the Marhøgda Bed at the southern margin of Van Keulenfjorden. A. BSE image showing kaolinite replacement structure encapsulating remnants of the original CFA. The grain occurs in phosphatic silty sandstone composed of quartz grains (Q) cemented by ultramicrocrystalline CFA (P), and containing framboidal pyrite (Fp). B, C. EDS spectra of CFA (B) and kaolinite (C) in the replaced grain.

pronounced variations in Mg and Ca contents (10.5–22.5 and 5.5–15.5 mol %, respectively; Fig. 13). Compositional changes are noted in samples from both the Marhøgda and Wimanfjellet sections, though without any general difference between the two locations. Mean composition of siderite in these sections is  $\text{Fe}_{0.75}\text{Mg}_{0.13}\text{Ca}_{0.12}\text{CO}_3$  and  $\text{Fe}_{0.74}\text{Mg}_{0.15}\text{Ca}_{0.11}\text{CO}_3$ , respectively.

Ankerite in the Marhøgda Bed at Sassenfjorden is a Fe-depleted (12–14 mol %  $\text{FeCO}_3$ ), Mn-poor (up to 0.3 mol %  $\text{MnCO}_3$ ) variety of ankerite (Figs 13, 14). Its mean composition in the Marhøgda and Wimanfjellet sections is  $\text{Ca}_{1.18}\text{Mg}_{0.56}\text{Fe}_{0.26}(\text{CO}_3)_2$ .

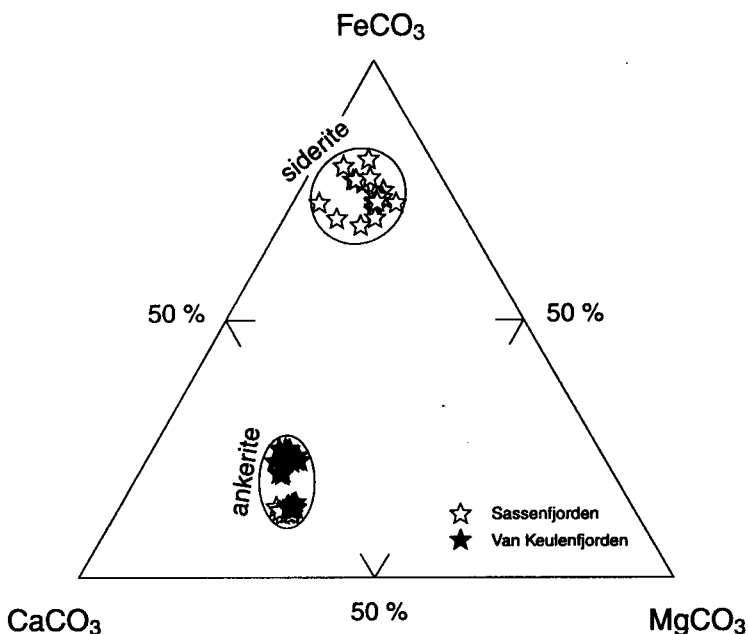


Fig. 13. Ternary diagram illustrating chemical composition of carbonate minerals in the Marhøgda Bed. Relative mol percentages of  $\text{FeCO}_3$ ,  $\text{CaCO}_3$ , and  $\text{MgCO}_3$ , recalculated for  $\text{MnCO}_3 = 0\%$ . Data from Tables 1–3

BSE images show that most of the ankerite is zoned, often on a scale of a single crystal (Fig. 15A, B). Detailed microprobe analysis indicates that the zonation reflects insignificant variation of iron, magnesium, and calcium contents in the mineral lattice (Fig. 15C). Manganese is virtually absent in cores of zoned ankerite crystals (zone Ak-1). It becomes detected in the first crystal ring encapsulating the core (zone Ak-2), with consequent increase of its contribution towards crystal margins (zones Ak-3 and Ak-4).

Ankerite in the Marhøgda Bed at Van Keulenfjorden shows two distinct chemical compositions (Figs 13, 14): (1) Fe-rich variety containing 20–26 mol %  $\text{FeCO}_3$  and 0.3–1 mol %  $\text{MnCO}_3$ , and (2) Fe-depleted, Mn-enriched variety containing 13–15 mol %  $\text{FeCO}_3$  and 2–3.5 mol %  $\text{MnCO}_3$ . Their mean composition is  $\text{Ca}_{1.06}\text{Mg}_{0.46}\text{Fe}_{0.47}\text{Mn}_{0.01}(\text{CO}_3)_2$  and  $\text{Ca}_{1.14}\text{Mg}_{0.53}\text{Fe}_{0.28}\text{Mn}_{0.05}(\text{CO}_3)_2$ , respectively. Fe-rich variety definitely prevails in the studied material. It has been noted in the two discerned morphologic types of ankerite, though it clearly dominates composition of large ankerite crystals (morphologic type 1). The two chemical varieties are approximately equally represented in smaller crystals forming concentric replacement zones, as well as in minute crystals occurring in kaolinite mosaics (morphologic type 2). Detailed microprobe analysis indicates that chemical composition of many ankerite crystals and aggregates changes on a microscale (Figs 16, 17). Cores of large ankerite crystals show predominantly Fe-rich, Mn-depleted compo-

Table 3

Chemical composition of ankerite in the Marhøgda Bed at the southern margin of Van Keulenfjorden

Van Keulenfjorden – chemical composition of ankerite (1)					
Location	Analysis	CaCO <sub>3</sub>	MgCO <sub>3</sub>	FeCO <sub>3</sub>	MnCO <sub>3</sub>
	mol %				
Ingebrigtsenbukta	1	52.52	23.32	23.55	0.61
	2	52.16	23.13	24.32	0.39
	3	52.08	23.12	24.40	0.40
	4	51.46	22.47	25.66	0.41
	5	54.43	22.52	22.11	0.94
	6	52.50	23.57	23.38	0.55
	7	51.60	24.80	23.27	0.33
	8	53.16	24.12	22.26	0.46
	9	50.80	24.14	24.24	0.82
	10	51.95	23.70	23.94	0.41
	11	51.47	22.97	24.91	0.65
	12	51.28	24.02	24.13	0.57
	13	53.59	20.75	25.30	0.36
	14	52.45	21.73	25.49	0.32
	15	51.67	22.62	25.16	0.55
	16	52.29	23.62	23.67	0.42
	17	55.48	21.02	22.91	0.59
	18	54.95	24.05	20.75	0.25
	19	56.16	23.20	20.23	0.41
	20	55.71	23.12	20.70	0.47

Van Keulenfjorden – chemical composition of ankerite (2)					
Location	Analysis	CaCO <sub>3</sub>	MgCO <sub>3</sub>	FeCO <sub>3</sub>	MnCO <sub>3</sub>
	mol %				
Ingebrigtsenbukta	1	56.75	27.17	13.68	2.41
	2	56.99	26.44	13.83	2.74
	3	57.42	26.70	14.09	1.79
	4	56.83	26.40	13.80	2.97
	5	56.85	27.01	13.91	2.23
	6	57.11	25.98	14.17	2.74
	7	56.41	25.54	14.63	3.42
	8	57.82	25.43	14.39	2.36
	9	57.24	26.23	14.66	1.87
	10	55.57	27.08	14.91	2.44

sition (zone Ak-1), whereas their thin external zone is usually composed of Fe-depleted, Mn-enriched chemical variety (zone Ak-2). Compositional changes at the boundary between the zones are abrupt, associated with an increase of MnCO<sub>3</sub> of about 2 mol % and a decrease of FeCO<sub>3</sub> content of about 10 mol %. Zonation of small ankerite crystals is usually hardly visible under TLM and in BSE images, though their chemical composition is also variable. Their cores are usually Fe-rich and Mn-depleted, with increasing content of Mn and decreasing content of

Table 4

Compositional changes in ankerite crystal in the Marhøgda Bed at Wimanfjellet (Sassenfjorden). Ak-1, Ak-2, Ak-3, and Ak-4 are crystal zones shown in Fig. 15

Sassenfjorden – compositional changes in ankerite crystals					
Crystal zone	Analysis	CaCO <sub>3</sub>	MgCO <sub>3</sub>	FeCO <sub>3</sub>	MnCO <sub>3</sub>
	mol %				
Ak-1	1	59.42	27.36	13.22	–
	2	59.48	27.52	13.00	–
Ak-2	3	59.23	28.62	12.09	0.06
	4	58.76	28.85	12.20	0.18
Ak-3	5	58.71	27.01	14.03	0.26
Ak-4	6	59.52	27.66	12.48	0.34
	7	58.50	28.43	12.72	0.35

Table 5

Compositional changes in ankerite crystals in the Marhøgda Bed at Ingebrigtsenbukta (Van Keulenfjorden). Ak-1, and Ak-2 are crystal zones shown in Figs 16 and 17

Van Keulenfjorden – compositional changes in ankerite crystals					
Crystal zone	Analysis	CaCO <sub>3</sub>	MgCO <sub>3</sub>	FeCO <sub>3</sub>	MnCO <sub>3</sub>
	mol %				
<b>Profile 1</b>					
Ak-2	1	56.27	26.06	15.66	2.01
	2	57.36	25.50	15.68	1.46
Ak-1	3	54.39	26.36	18.26	0.99
	4	53.64	21.30	24.46	0.60
	5	52.92	22.50	24.16	0.42
	6	51.26	23.23	24.94	0.42
	7	51.83	22.69	24.81	0.67
	8	53.02	22.37	24.14	0.47
	9	54.38	21.45	23.80	0.37
	10	52.30	21.89	25.16	0.65
	11	53.56	25.13	20.57	0.74
Ak-2	12	55.43	27.19	14.88	2.50
<b>Profile 2</b>					
Ak-1	1	52.67	28.48	18.10	0.75
	2	51.47	23.33	24.61	0.59
	3	51.97	21.69	25.47	0.87
	4	51.81	23.30	24.64	0.25
	5	51.71	23.08	24.70	0.51
	6	53.27	28.47	17.25	1.01
Ak-2	7	57.13	26.46	14.43	1.98
	8	57.01	26.18	14.52	2.29
<b>Profile 3</b>					
hardly discerned	1	54.87	28.07	14.72	2.34
	2	51.56	31.97	15.06	1.41
	3	54.26	26.39	17.79	1.56
	4	52.12	27.01	20.09	0.78
	5	56.01	27.06	16.00	0.93
	6	55.35	26.47	16.14	2.04
	7	56.87	26.47	13.56	3.10

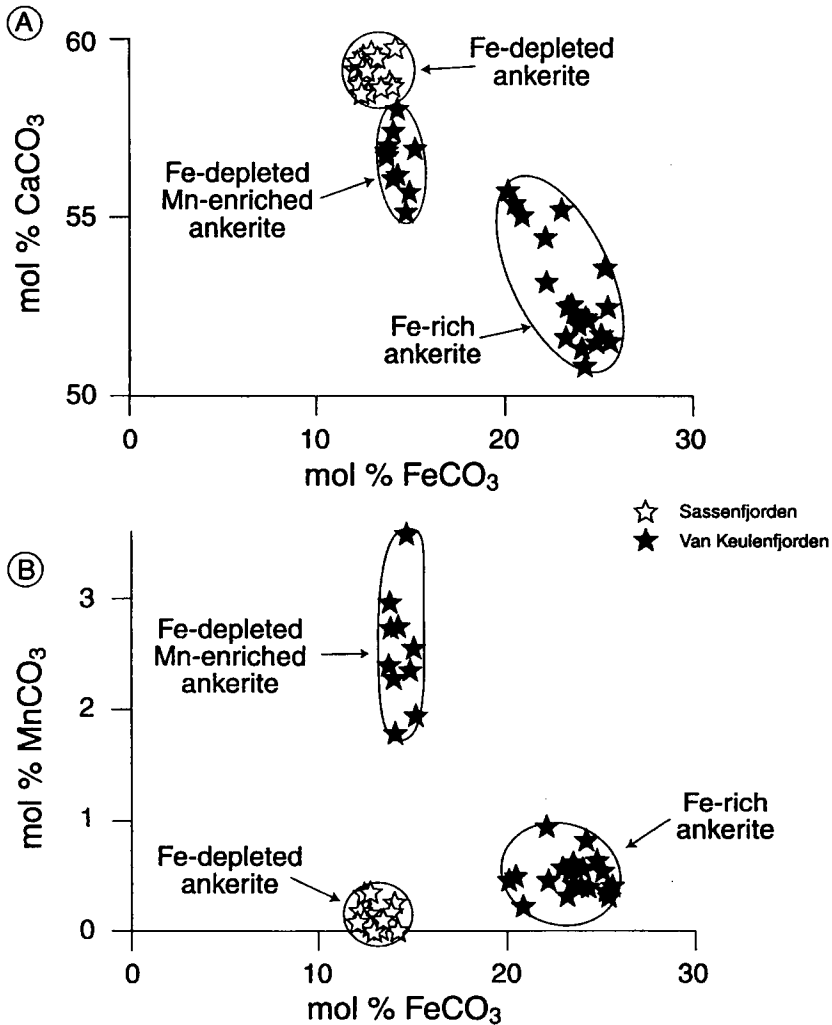


Fig. 14. A. Mol % FeCO<sub>3</sub> versus mol % CaCO<sub>3</sub> content in ankerite in the Marhøgda Bed. B. Mol % FeCO<sub>3</sub> versus mol % MnCO<sub>3</sub> content in ankerite in the Marhøgda Bed. Data from Tables 1–3

Fe towards crystal margins. This suggests that Fe-rich ankerite was precipitated earlier than the Fe-depleted one, and is consistent with petrographic observations.

### Carbon and oxygen isotopes

The obtained  $\delta^{13}\text{C}$  and  $\delta^{18}\text{O}$  values for carbonate minerals present in the Marhøgda Bed are listed in Table 6.

Siderite in the Marhøgda Bed at Sassenfjorden has  $\delta^{13}\text{C}$  values between  $-9.0$  and  $-5.7$  ‰, without any clear difference between the Marhøgda and Wimanfjellet sections (Fig. 18). Ankerite at Sassenfjorden falls in the middle of the sideritic

Table 6  
Carbon and oxygen isotopic composition of carbonate minerals in the Marhøgda Bed

Marhøgda Bed – isotopic composition of carbonate minerals							
Sample		20h	48h	96h	120h	168h	120h (25°C)
		(25°C)					4h (100°C)
% VPDB							
Marhøgda M-1	$\delta^{13}\text{C}$				-7.08	-7.49	-8.40
	$\delta^{18}\text{O}$				-8.90	-4.18	-3.01
Marhøgda M-2	$\delta^{13}\text{C}$	-6.92			-6.72	-6.31	-7.68
	$\delta^{18}\text{O}$	-8.88			-8.60	-3.59	-2.50
Wimanfjellet W-1	$\delta^{13}\text{C}$				-7.54	-7.29	-8.97
	$\delta^{18}\text{O}$				-4.34	-2.32	-1.42
Wimanfjellet W-2	$\delta^{13}\text{C}$	-7.18			-6.63	-5.66	-7.30
	$\delta^{18}\text{O}$	-8.20			-7.41	-3.11	-1.87
Ingebrigtsenbukta I-1	$\delta^{13}\text{C}$			-7.96			
	$\delta^{18}\text{O}$			-11.41			
Ingebrigtsenbukta I-2	$\delta^{13}\text{C}$	-7.62	-7.86				
	$\delta^{18}\text{O}$	-11.46	-10.49				

range (-7.5 to -6.6 ‰). Ankerite at Van Keulenfjorden has slightly more negative values between -7.9 and -7.6 ‰.

Siderite and ankerite show a pronounced difference in the oxygen isotopic composition (Fig. 19). Siderite at Sassenfjorden has  $\delta^{18}\text{O}$  values between -4.2 and -1.4 ‰ VPDB, whereas the co-existing ankerite is noticeably depleted in  $^{18}\text{O}$  (-8.9 to -7.4 ‰). Only one sample in the Wimanfjellet section (W-1) gave anomalously high ankeritic value of -4.3 ‰. Ankerite at Van Keulenfjorden is even more depleted in  $^{18}\text{O}$ , with  $\delta^{18}\text{O}$  ranging from -11.5 to -10.5 ‰.

## Discussion

Petrographic, geochemical, and stable carbon and oxygen isotopic data indicate that the carbonates in the Marhøgda Bed do not represent depositional limestone facies, but diagenetic mineral suite that originated at base of organic-rich sediment column of the Agardhfjellet Formation. Siderite and, to a lesser extent, ankerite are the most volumetrically important diagenetic carbonate minerals in this lithostratigraphic unit. The abundance of Fe-rich carbonates is typical of the Agardhfjellet Formation (Dypvik 1978, Krajewski 1992a, Bausch *et al.* 1998, Mørk *et al.* 1999), and probably results from an abundance of reactive iron in organic-rich facies in Late Jurassic sedimentary basin in Svalbard.

The recognition and characterization of diagenetic mineral sequence allows for reconstruction of post-depositional history of the Marhøgda Bed. Two episodes of carbonate diagenesis, including early siderite precipitation and burial formation of ankerite, seem to have contributed to the development of this cementstone band.

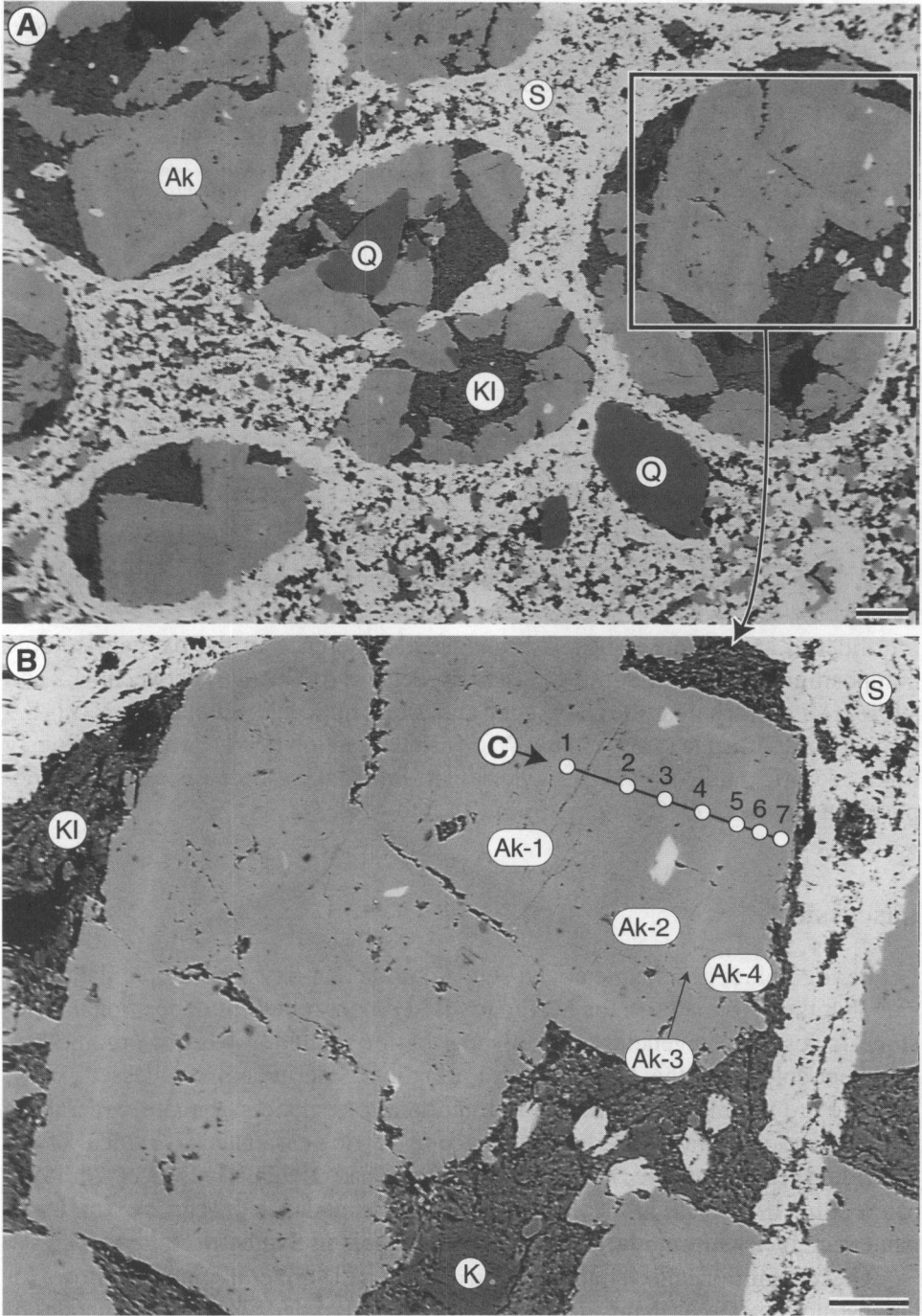


Fig. 15.

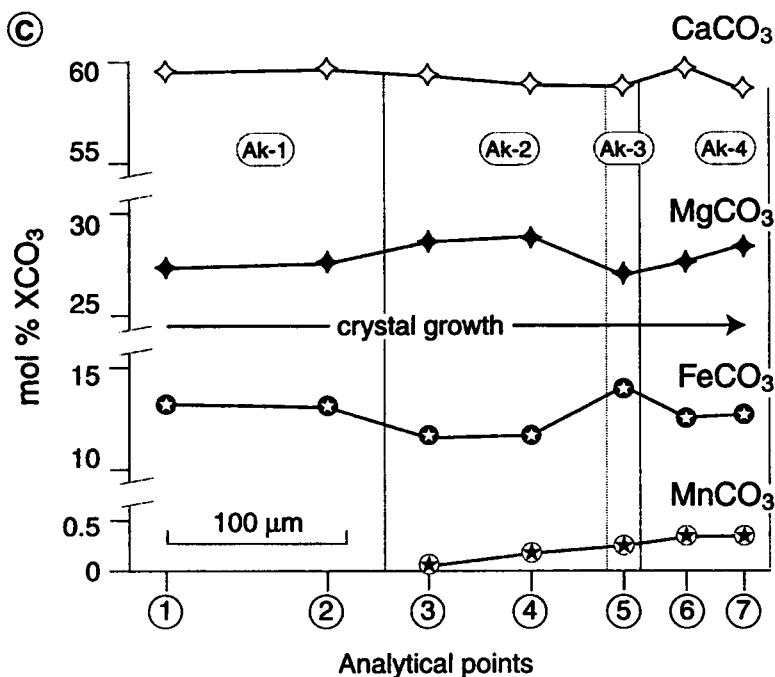


Fig. 15 (continued). Compositional changes in ankerite crystals in the Marhøgda Bed at the southern margin of Sassenfjorden. A. BSE image of replaced glauconite pellets and phosphatic ooids in sideritic matrix (*S*) of the Marhøgda Bed in the Wimanfjellet section. The replacement structures consist of large, zoned ankerite crystals (*Ak*) and kaolinite–illite mosaics (*KI*). Quartz grains (*Q*) occur both in the matrix and in replaced grains. B. Zoned ankerite crystals in replaced glauconite pellet composed of kaolinite–illite mosaic (*KI*) encapsulating vermicular aggregates of pure kaolinite (*K*). The matrix consists of minute, interlocking siderite crystals (*S*), and similar siderite crystals occur scattered in the replacement structure. *Ak-1* to *Ak-4* are crystal zones developed during consequent stages of ankerite precipitation. 1 to 7 are analytical points along EDS quantitative compositional profile shown in C. A, B: scale bars = 100  $\mu\text{m}$ . C. Compositional changes in zoned ankerite crystal along EDS profile shown in B. Data from Table 4.

### Timing of carbonate precipitation

Determination of the relative timing of carbonate precipitation in the Marhøgda Bed is important in the interpretation of its diagenetic origin. Possible lines of evidence embrace reconstruction of the precipitation sequence from petrographic observations and geochemical analysis, as well as from the carbon and oxygen isotopic record.

**Constraints from mineral sequence.** — Petrographic examination of the Marhøgda Bed in its type locality at the southern margin of Sassenfjorden revealed no evidence for replacement of a depositional limestone precursor. The matrix-forming siderite appears to have formed entirely through direct precipitation in intergranular pores of originally fine-grained, porous sediment composed of

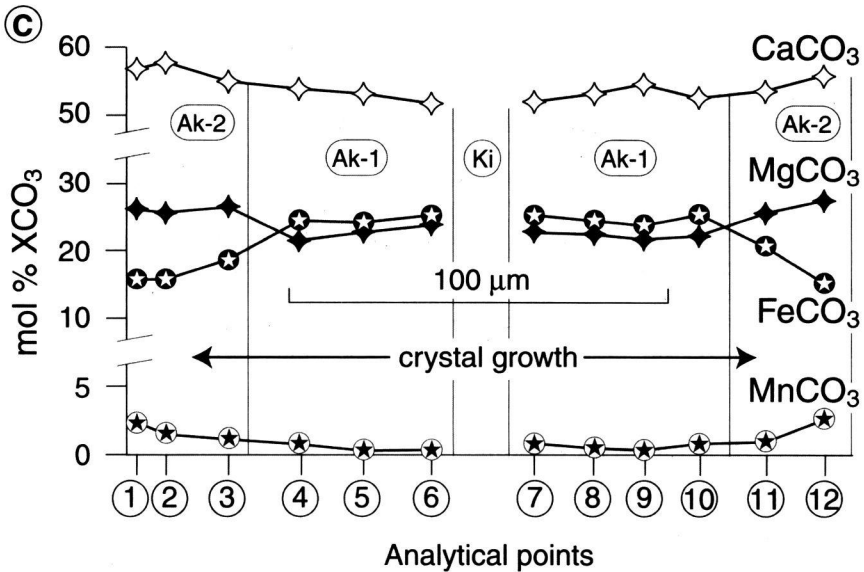
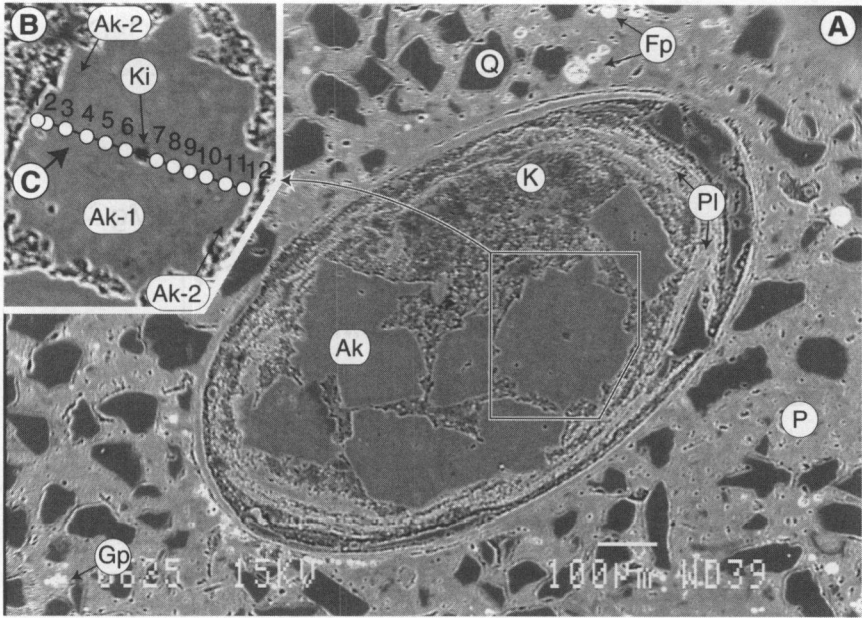


Fig. 16. Compositional changes in ankerite crystals in the Marhøgda Bed at the southern margin of Van Keulenfjorden (I). A. BSE image of large subhedral to anhedral ankerite crystals (Ak) and kaolinite mosaic (K) replacing phosphatic ooid composed of laminated, ultramicrocrystalline CFA (PI). The ooid occurs in phosphatic silty sandstone composed of quartz grains (Q) cemented by ultramicrocrystalline CFA (P), and containing framboidal (Fp) and microgranular pyrite (Gp). B. Ankerite crystal containing small kaolinite inclusion in its centre (Ki) consists of a thick core (Ak-1) rimmed by thin external crystal zone (Ak-2). 1 to 12 are analytical points along EDS quantitative compositional profile shown in C. C. Compositional changes in zoned ankerite crystal along EDS profile shown in B. Data from Table 5.

clay minerals and fine clastic and phosphatic particles. This sediment contained abundant glauconite pellets and phosphatic ooids and grains that were concentrated above the Brentskardhaugen Bed under intermittent hiatal conditions during the initial stage of the Agardhfjellet shale deposition.

Typical diagenetic sequence in organic-rich marine sediment column is defined by dominant microbiological processes involved in organic matter decomposition (Berner 1981, Maynard 1982, Curtis 1987, Canfield 1994). It includes surficial oxic zone (OX-zone) underlain by suboxic zone (the latter is commonly defined by microbial reduction of iron, and referred to as iron reduction zone or FeR-zone), anoxic sulphidic or sulphate reduction zone (SR-zone), and zone of microbial methanogenesis (Me-zone). Deeper diagenetic environments are defined by abiotic reactions, including thermally-induced decarboxylation (D-zone). Formation of siderite requires supply, at a sufficient rate, of  $\text{Fe}^{2+}$  ions to the pore water due mostly to reductive dissolution of ferric iron compounds. Since  $\text{Fe}^{2+}$  ions in the SR-zone are preferentially precipitated as iron sulphides and pyrite (Coleman 1985, Gautier 1985), extensive siderite formation may occur either in shallower (FeR-zone) or deeper (Me- and D-zones) diagenetic environments (Maynard 1982, Curtis and Coleman 1986).

Early diagenetic nature of siderite in the Marhøgda Bed points to the FeR-zone as a principal environment of the mineral formation. Extremely rare early diagenetic pyrite noted in the Marhøgda Bed at Sassenfjorden suggests that nearly all easily metabolizable iron was exhausted before anoxic sulphidic conditions became dominant in the sediment. The sideritic matrix in the Marhøgda Bed shows striking petrographic similarities to other early diagenetic sideritic cementstones originated in the FeR-zone zone of organic-rich sediments (Mozley and Carothers 1992, Huggett *et al.* 2000). The impure, Mg- and Ca-enriched nature of the siderite is typical for early diagenetic siderites from marine depositional environments and probably reflects low  $\text{Fe}^{2+}/\text{Mg}^{2+}$  and  $\text{Fe}^{2+}/\text{Ca}^{2+}$  ratios of early marine pore waters (Curtis and Coleman 1986, Mozley 1989a, b). The low Mn content is also typical for early diagenetic siderites (Mozley and Carothers 1992). The amount of Mg and Ca is variable, and probably influenced by the concentrations of  $\text{Fe}^{2+}$ ,  $\text{Mg}^{2+}$ , and  $\text{Ca}^{2+}$  in the pore waters from which it precipitated (Matsumoto and Iijima 1981).

The apparent lack of early siderite formation in oolitic siltstone of the Marhøgda Bed at Van Keulenfjorden was coupled with common precipitation of early pyrite accompanied by pyritization of organic matter. This suggests that dissimilatory sulphate reduction in the SR-zone became a dominant early diagenetic process of organic matter decomposition in the area. It also suggests that microbial reduction of iron in the FeR-zone was inefficient or too short lasting to produce sufficient concentration of  $\text{Fe}^{2+}$  ions for extensive siderite precipitation.

Petrographic observations indicate that ankerite post-dated early siderite formation in the Marhøgda Bed at Sassenfjorden. Zoned nature of anhedral to subhedral ankerite crystals replacing the original glauconite/phosphate grains suggests their late diagenetic development under burial conditions in the Agardhfjellet Formation.

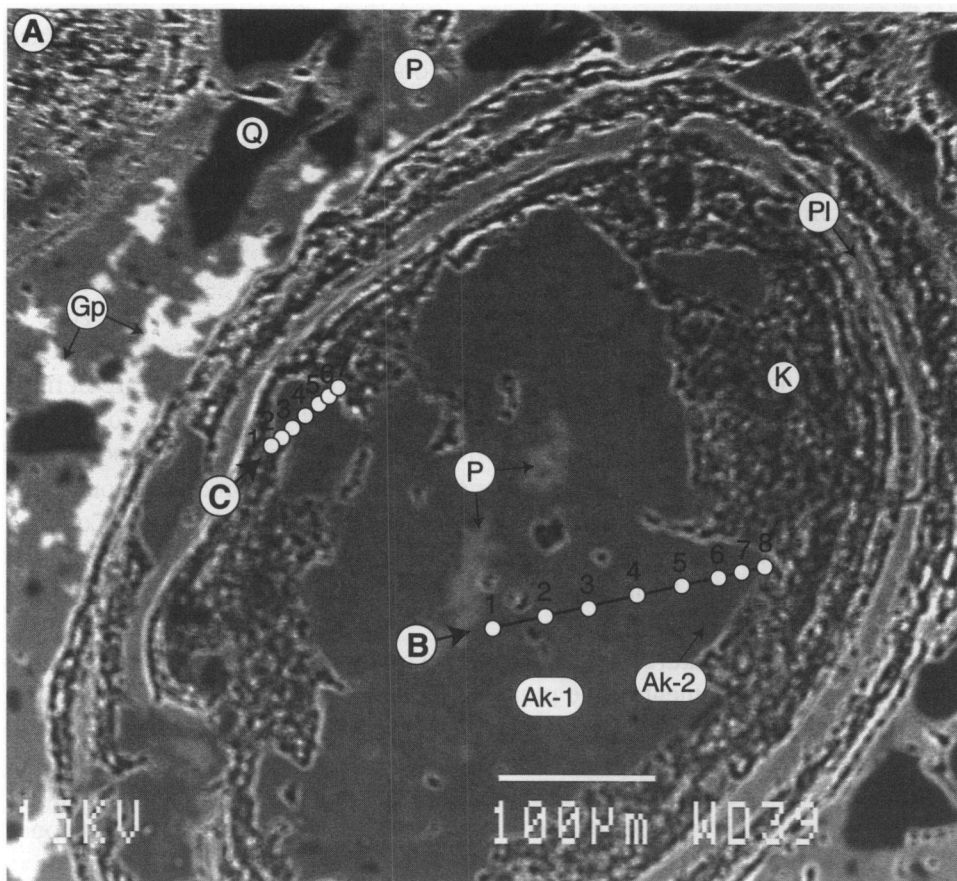


Fig. 17. Compositional changes in ankerite crystals in the Marhøgda Bed at the southern margin of Van Keulenfjorden (II). A. BSE image of ankerite crystals and kaolinite mosaic (*K*) replacing phosphatic ooid composed of laminated, ultramicrocrystalline CFA (*PI*). The ooid occurs in phosphatic silty sandstone composed of quartz grains (*Q*) cemented by ultramicrocrystalline CFA (*P*), and containing microgranular pyrite (*Gp*). Large ankerite crystal in the centre contains irregular remnants of the original phosphatic fabric (*P*), and consists of a thick core (*Ak-1*) rimmed by thin external crystal zone (*Ak-2*). Small ankerite crystal to the left hardly shows any zonation. 1 to 8 and 1 to 7 are analytical points along EDS quantitative compositional profiles shown in *B* and *C*, respectively.

Ankerite in the Marhøgda Bed at Van Keulenfjorden is also preferentially developed in phosphatic ooids and grains, suggesting similar diagenetic origin.

Calcium, magnesium and iron for ankerite precipitation are likely to have been derived from mineral transformations and dissolution during burial of the Agardhfjellet Formation. Ankerite-replaced skeletal remains witness dissolution of biogenic calcite. Iron and magnesium are likely to have been derived from transformations of glauconite and other clay minerals as well as from reductive dissolution of ferric iron compounds that escaped microbial reduction in surficial diagenetic zones. Ankerite in the Marhøgda Bed at Sassenfjorden is Fe-depleted, suggesting

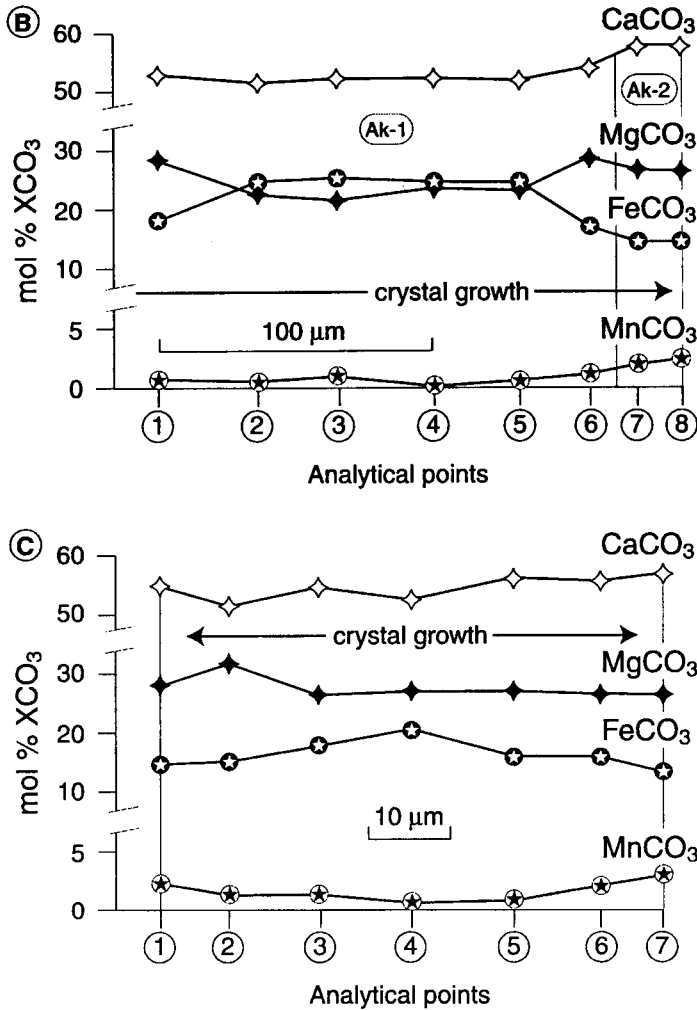


Fig. 17. (continued) B, C. Compositional changes in ankerite crystals along EDS profiles shown in A. Data from Table 5.

that Fe<sup>2+</sup> release to the pore fluids was limited by the availability of iron-containing mineral phases that transformed during burial diagenesis. This is consistent with the abundance of early siderite that fixed easily reducible iron in the sequence, and with late diagenetic alteration of glauconite. Mn<sup>2+</sup> cations appeared in the pore fluids during the ankerite formation, and became noticeable component during later stages of mineral precipitation, suggesting an increased release of manganese during burial of the Agardhfjellet Formation in central Spitsbergen.

Fe-rich ankerite represents the first and dominant burial carbonate phase in the Marhøgda Bed at Van Keulenfjorden, suggesting its precipitation under conditions of accelerated liberation of Fe<sup>2+</sup> cations to the pore fluids of the Agardhfjellet For-

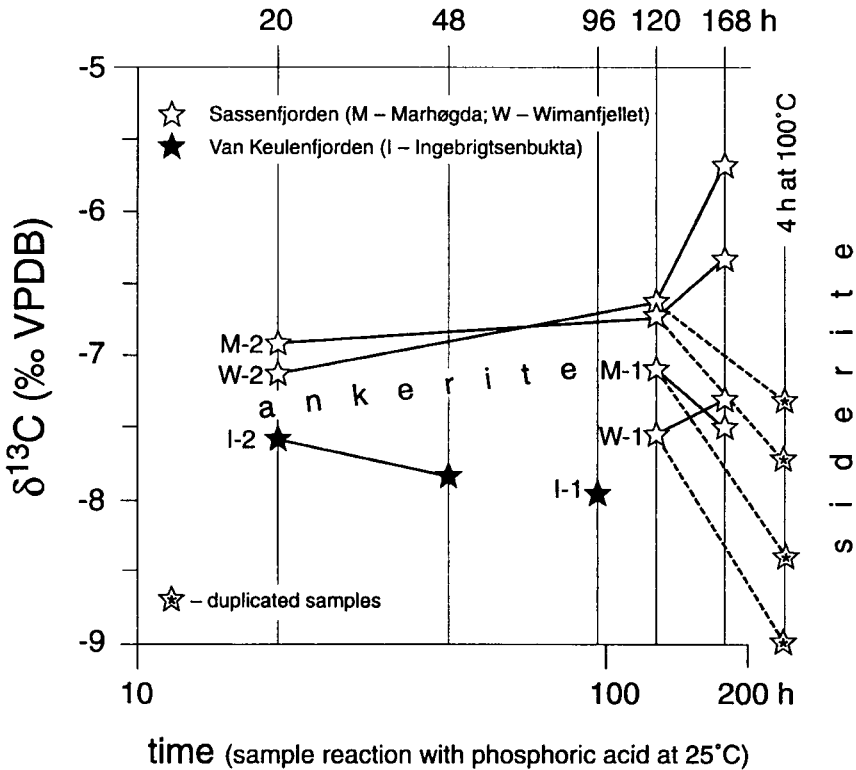


Fig. 18. Carbon isotopic composition of carbonate minerals in the Marhøgda Bed. Data from Table 6.

mation in the Bellsund area. Subsequent ankerite is Fe-depleted and Mn-enriched, suggesting mineral precipitation during enhanced liberation of  $\text{Mn}^{2+}$  cations after the major iron source became partly exhausted.

**Constraints from  $\delta^{13}\text{C}$ .** — Marine carbonate rocks normally have  $\delta^{13}\text{C}$  compositions of about  $0 \pm 3\text{‰}$  (VPDB), as do cements derived by dissolution of pre-existing depositional carbonates (Longstaffe 1983, Lundegard and Land 1986). The  $\delta^{13}\text{C}$  values of carbonate minerals in the Marhøgda Bed ( $-9$  to  $-6\text{‰}$ ) are considerably lower, suggesting that they did not originate from recrystallization of a depositional lime sediment, but represent diagenetic mineral phases precipitated from fluids in which biogenic carbon dioxide was an important component.

Carbonate cements and concretions in marine organic-rich rocks have  $\delta^{13}\text{C}$  compositions in a broad range from approx.  $-30$  up to  $+30\text{‰}$  (Mozley and Burns 1993, Scotchman 1989, Thornburg and Suess 1990), reflecting their formation at different diagenetic zones in sediment columns under consequent steps of organic matter decomposition and production of biogenic carbon dioxide (Claypool and Kaplan 1974, Irwin *et al.* 1977, Coleman 1985). Processes that control isotopic composition of carbonate carbon in these diagenetic environments include: (1) carbonate derived from

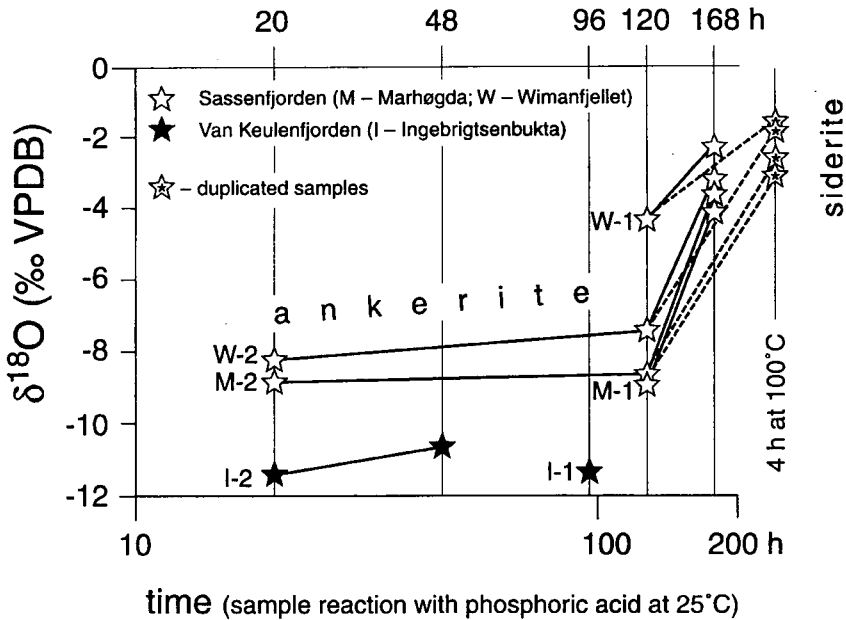


Fig. 19. Oxygen isotopic composition of carbonate minerals in the Marhøgda Bed. Data from Table 6.

oxidation of marine organic matter in the OX-, FeR- and SR- diagenetic zones ( $\delta^{13}\text{C} \approx -25\text{‰}$ ); (2) dissolved carbonate in marine pore waters ( $\delta^{13}\text{C} \approx 0 \pm 3\text{‰}$ ); (3) carbonate derived from dissolution of marine skeletal carbonates ( $\delta^{13}\text{C} \approx 0 \pm 3\text{‰}$ ); (4) carbonate derived from microbial methanogenesis in the Me-zone ( $\delta^{13}\text{C}$  strongly variable, but up to approx.  $+20\text{‰}$ ); (5) carbonate originated as a result of oxidation of diffused methane at oxidation fronts in the OX-zone or in the SR-zone ( $\delta^{13}\text{C}$  strongly negative, down to approx.  $-80\text{‰}$ ); and (6) carbonate derived from thermally induced decarboxylation processes in the D-zone ( $\delta^{13}\text{C} \approx -20\text{‰}$ ).

The  $\delta^{13}\text{C}$  values of carbonate minerals in the Marhøgda Bed suggest that carbon was supplied in nearly equal amounts from mineral carbonate and organic carbon compounds for both the early (siderite) and late (ankerite) precipitates. This is consistent with the respective formation of these carbonates in the FeR- and D-zones, accompanied by a progressive dissolution of easily (aragonite) and less soluble (calcite) biogenic carbonate particles (Fig. 20). The apparent lack of carbonates precipitated in the Me-zone may suggest early kerogenization of organic fractions that escaped degradation during early stages of sediment diagenesis. Alternatively, it may suggest methanogenesis utilizing carbon dioxide reduction pathway, which is typical of marine sediment columns, and associated with  $\text{CO}_2$  removal from pore waters (Whiticar *et al.* 1986, Whiticar 1999).

**Constraints from  $\delta^{18}\text{O}$ .** — The oxygen isotope composition of carbonate minerals can be used to calculate their precipitation temperatures if the composition of

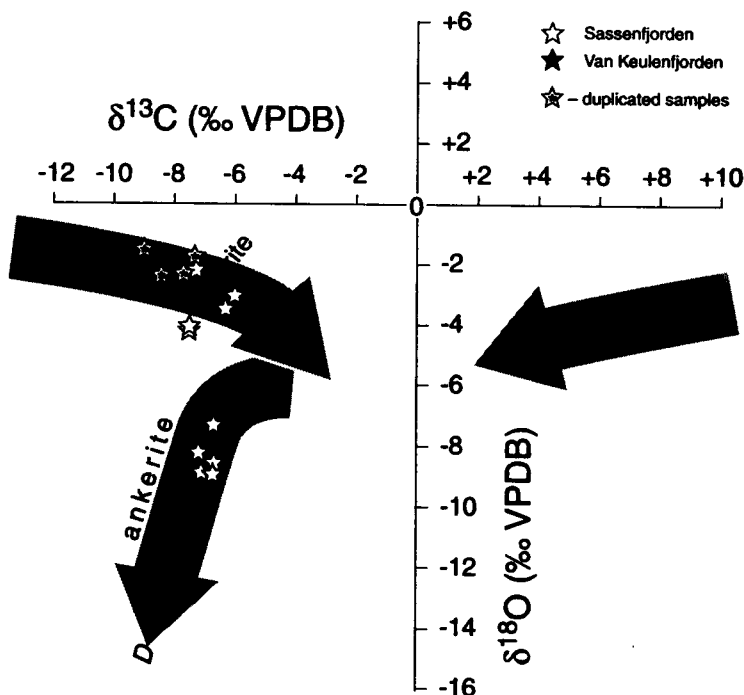


Fig. 20. Plot of  $\delta^{13}\text{C}$  (‰ VPDB) versus  $\delta^{18}\text{O}$  (‰ VPDB) of the Marhøgda carbonates. Diagenetic trends of carbonates formed in the iron reduction – sulphate reduction zones (*FeR* & *SR*-zones), methanogenic zone (*Me*-zone), and decarboxylation zone (*D*-zone) after Scotchman (1989).

precipitating water is known or assumed, and equilibrium relationships controlling  $\delta^{18}\text{O}$  are assumed (Fritz 1976). The outcome of these calculations ultimately depends upon the fractionation equation used.

To our knowledge there are no studies attempting to reconstruct oxygen isotopic composition of Jurassic seawater in Svalbard, neither there are studies dealing with evolution of Jurassic formation waters in the area. Our attempt to estimate precipitation temperatures of diagenetic carbonate minerals in the Marhøgda Bed employs a range of possible  $\delta^{18}\text{O}$  compositions of coeval seawater (–5 to 0 ‰ SMOW), and assumes stagnant burial regime without important  $\delta^{18}\text{O}$  changes of the pore waters.

Early diagenetic, Mg- and Ca-enriched siderite in the Marhøgda Bed at Sassenfjorden has oxygen isotopic composition in a narrow range, suggesting its formation as a result of single episode of mineral precipitation. Precipitation temperatures calculated using the equation for microbial Mg/Ca siderite (Mortimer and Coleman 1997) and the range of compositions of seawater are between 4 and 28°C (Fig. 21), i.e. within the limits of sedimentary temperatures. This agrees with petrographic observations suggesting early siderite precipitation in nearsurface FeR-zone of organic-rich sediment. Assuming that isotopic composition of Jurassic

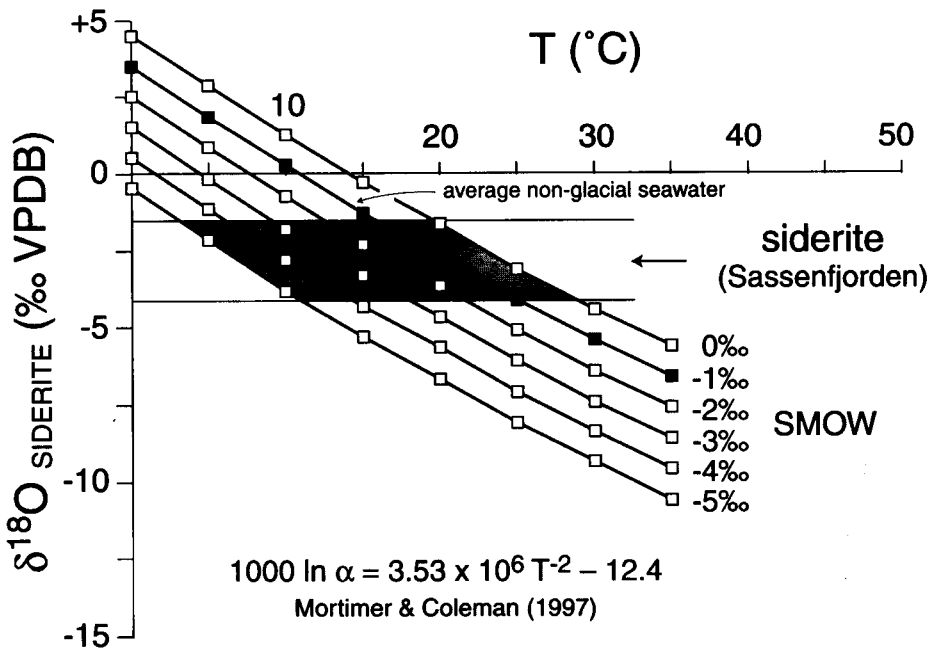


Fig. 21. Range of  $\delta^{18}\text{O}$  values (‰ VPDB) of the Marhøgda siderite against precipitation temperature  $T$  ( $^{\circ}\text{C}$ ) of microbial siderite, with the calculated isotopic composition of early diagenetic fluids from which it may have formed, assuming isotopic equilibrium. The water lines were calculated using the fractionation equation of Mortimer and Coleman (1997) for microbial Mg/Ca siderite.

seawater in Svalbard was close to average non-glacial seawater ( $-1$  ‰ SMOW), the calculated temperatures fall between 15 and 25 $^{\circ}\text{C}$ . The lower limit of this temperature range corresponds to postulated ambient sea water temperatures during deposition of the Agardhfjellet Formation (P. Ditchfield in Harland 1997, p. 381). It is also close to the calculated temperatures from the Middle–Late Jurassic belemnites in Kong Karls Land (9.4–12.7 $^{\circ}\text{C}$ ), given a non-glacial sea water composition of  $-1$  ‰ SMOW (Ditchfield 1997).

Diagenetic ankerite in the Marhøgda Bed has strongly negative  $\delta^{18}\text{O}$  values. As petrographic observations suggest burial diagenetic formation of the ankerite, it is possible to interpret its oxygen isotope values in terms of temperature controls associated with depth of burial. However, because the ankerite shows wide compositional variations, equilibrium isotopic fractionation between ankerite and pore water for a given temperature might also vary. In our temperature calculations, we used two different fractionation equations to account for compositional variations, i.e. the equation of Land (1985) for inorganic dolomite, and the one of Fisher and Land (1986) for inorganic ankerite. The results are shown in Fig. 22A and B, respectively.

Precipitation temperatures calculated for the Marhøgda ankerite at Sassenfjorden fall in a range between 50–100 $^{\circ}\text{C}$  and 40–90 $^{\circ}\text{C}$  (for assumed  $\delta^{18}\text{O}_{\text{pore water}}$

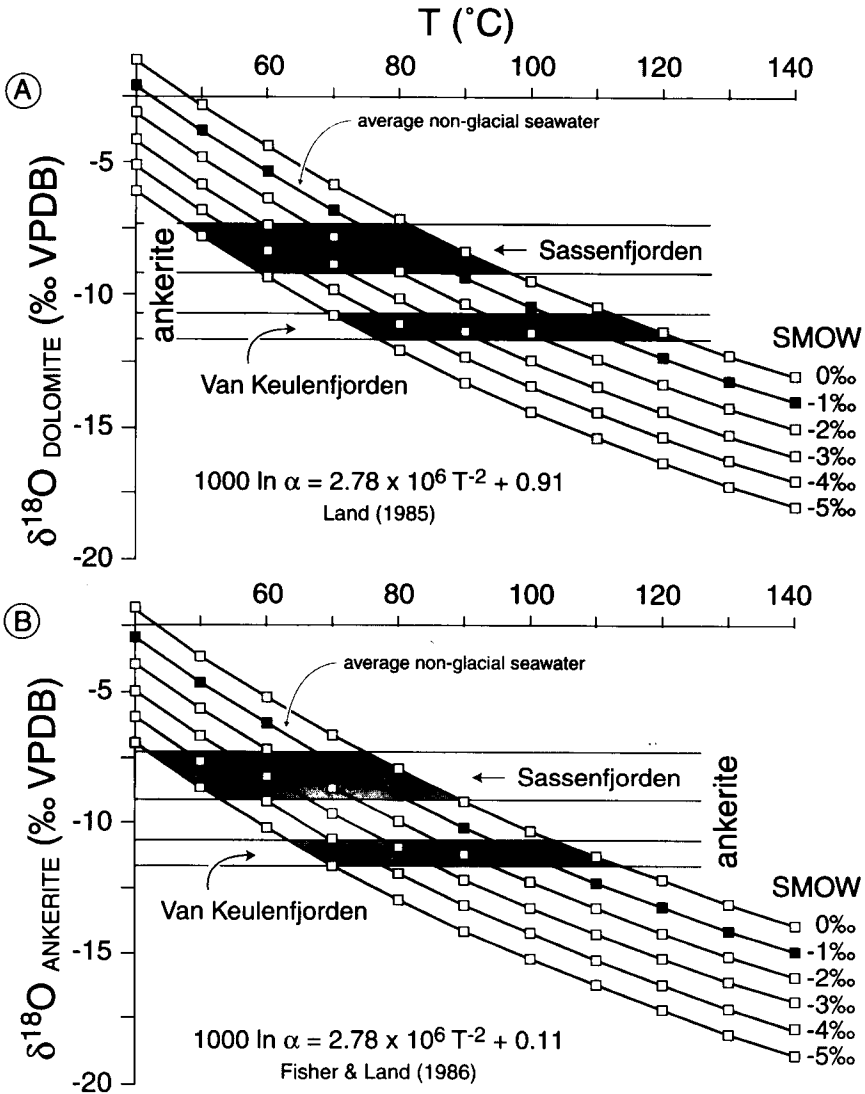


Fig. 22. Range of  $\delta^{18}\text{O}$  values (‰ VPDB) of the Marhøgda ankerite against precipitation temperature  $T$  (°C) of inorganic dolomite (A) and ankerite (B), with the calculated isotopic composition of diagenetic fluids from which it may have formed, assuming isotopic equilibrium. The water lines were calculated using the fractionation equation of Land (1985) for dolomite, and the equation of Fisher and Land (1986) for ankerite.

from  $-5$  to  $0$  ‰ SMOW), depending on whether dolomite-water or ankerite-water isotopic fractionation expression is used. For isotopic composition of pore water with assumed average value of non-glacial seawater ( $-1$  ‰ SMOW), the calculated temperature range is between approx.  $80$ – $90$ °C and  $70$ – $80$ °C, respectively. The difference of  $3$ – $4$  ‰  $\delta^{18}\text{O}$  between ankerite at Sassenfjorden and at Van

Keulenfjorden corresponds to a temperature difference of about 20°C, regardless of which fractionation expression is used. Higher precipitation temperatures at Van Keulenfjorden (100–110°C and 90–100°C for  $\delta^{18}\text{O}_{\text{pore water}} = -1\text{‰ SMOW}$ ) correlate with a general increase in the content of  $\text{Fe}^{2+}$  and  $\text{Mn}^{2+}$  cations in the ankerite lattice, as compared to Sassenfjorden. This suggests local changes in geochemistry of formation waters in the Agardhfjellet Formation, reflecting probably differences in the availability of reducible iron and manganese mineral phases in the shale sequence.

The estimated mean temperatures of ankerite precipitation (about 80–100°C) roughly correspond to those at which carboxylic acid anions released during thermal decomposition of kerogen become important components in pore waters (Means and Hubbard 1987, Lundegard and Kharaka 1990, Lewan and Fisher 1994). They are also within the temperature window at which these acid anions break down as a result of thermal decarboxylation (Drummond and Palmer 1986, Kharaka *et al.* 1986). Similar temperatures have been revealed for several burial ankerites, suggesting that this carbonate is typical for thermal decarboxylation environments in organic-rich marine sedimentary sequences (e.g., Fisher and Land 1986, Hendry *et al.* 2000). Zoned nature of ankerite at Sassenfjorden and the presence of two ankerite generations at Van Keulenfjorden suggest that the mineral precipitated during prolonged period of time under changing burial conditions. The estimated temperatures should therefore reflect mean value ranges from broader ranges recording burial histories of mineral precipitation in the sequence.

The Agardhfjellet Formation at Sassenfjorden and at Van Keulenfjorden is approximately 200 and 300 m thick, respectively (Różycki 1959, Dypvik *et al.*, 1991a, b, Bausch *et al.* 1998, Mørk *et al.* 1999). The estimated temperatures of ankerite precipitation correspond to burial depths far greater than the ones attained during or directly after the deposition of the Agardhfjellet Formation, whatever a probable geothermal gradient is assumed. This suggests ankerite precipitation upon burial under the overlying sedimentary formations during the post-Jurassic geological history of Spitsbergen. Basic magmatic event at the Jurassic/Cretaceous boundary (Harland 1997) affected locally thermal alteration of kerogen in the Agardhfjellet Formation (Birkenmajer 1979), though the importance of this process in mineral precipitation is difficult to assess on the basis of material analyzed here.

### Diagenetic stability of glauconite and CFA

Petrographic data suggest that glauconite and CFA grains in the Marhøgda Bed passed through early stages of diagenesis without any important mineral transformations, whatever siderite or pyrite formation dominated the early diagenetic system. Rare siderite crystals in glauconite/phosphate grains at Sassenfjorden and single pyritic framboids in phosphatic ooids at Van Keulenfjorden suggest diagenetic precipitation in the original porous structure of the grains, rather than mineral replacement.

Advanced alteration and dissolution of glauconite and CFA began during burial diagenesis, and was associated with increased temperatures, thermal alteration of kerogen, and precipitation of ankerite. Alteration of glauconite consisted in both iron removal from the mineral structure and the mineral dissolution and precipitation of kaolinite. The two processes seem to have operated in consort, even on a scale of a single pellet. Secondary products include various mixtures of illite and kaolinite containing inclusions and vermicular aggregates of pure kaolinite. Detailed EDS investigation suggests that kaolinitization of clay minerals also occurred in matrix of the Marhøgda Bed.

Phosphatic ooids and grains preserved at various stages of diagenetic alteration suggest that CFA was dissolved before and during formation of their replacement structures. Since phosphatic grains originally had no or subordinate clay admixture, diagenetic clay cement occurring in their replacement structures is almost entirely pure kaolinite. Ankerite precipitation in these grains seems to have slightly preceded the precipitation of kaolinite. Burial dissolution of CFA provided dissolved phosphate to the pore waters, and might contribute to formation of secondary apatite in the basal part of the Agardhfjellet Formation. No secondary apatite has been revealed in the Marhøgda Bed, though documentation of its occurrence requires systematic petrographic investigation that exceeds the material analyzed for the scope of this paper. It should be noted that secondary CFA fabrics associated with kaolinite cements have been revealed in the underlying Brentskardhaugen Bed (Krajewski 2001).

### Controls on the Marhøgda cementstone development

The well-developed cementstone band of the Marhøgda Bed at Sassenfjorden owes its origin to early cementation by siderite, most probably in the FeR diagenetic zone. Early carbonate cementation in the Marhøgda Bed was of far less importance at Van Keulenfjorden, suggesting differences in the nature and intensity of early diagenetic processes during initial stage of the Middle–Late Jurassic drowning of the Svalbard shelf. Possible controls on the course of early diagenesis in the two areas embrace differences in bottom water oxygenation and in sedimentation rate during the deposition of basal sediments of the Agardhfjellet Formation (Fig. 23). The black, organic-rich laminated shale at Van Keulenfjorden (informal Ingebrigtsenbukta member of Mørk *et al.* 1999) appears just above the Brentskardhaugen/Marhøgda horizon (Różycki 1959, Krajewski, 1992a), whereas at Sassenfjorden the organic-rich shale of the Lardyfjellet Member is separated from the horizon by a sequence of grey bioturbated siltstone, mudstone, and shale of the Oppdalen Member showing depletion in organic carbon content (Krajewski 1989, Dypvik *et al.* 1991a, b, Mørk *et al.* 1999). This suggests shallower depositional environment, higher level of oxygenation of bottom water and perhaps lower sedimentation rates at base of the Agardhfjellet Formation in the Sassenfjorden area, as compared to the Van Keulenfjorden area. Oxygenation of bottom water and decel-

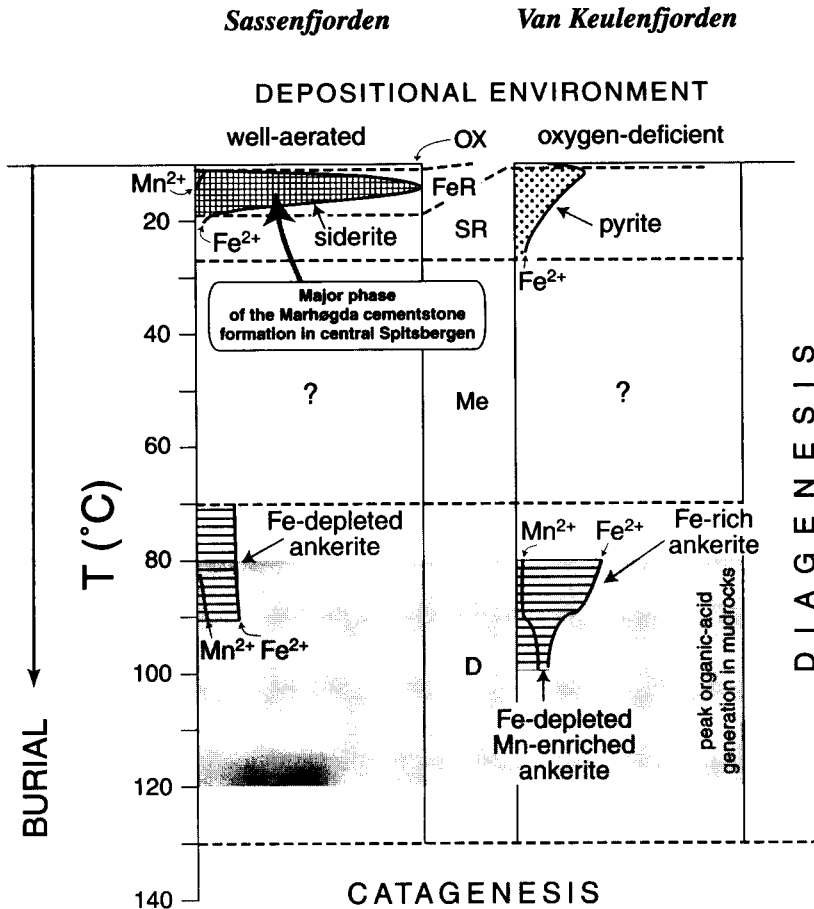


Fig. 23. Diagenetic history the Marhøgda Bed at Sassenfjorden and Van Keulenfjorden against burial temperatures and relative availability of iron and manganese cations in pore fluids. OX, FeR, SR, Me, and D are oxic, iron-reduction, sulphate-reduction, methanogenic, and thermal decarboxylation diagenetic zones, respectively. Temperature range of peak organic-acid generation after Hendry *et al.* (2000).

erated sedimentation rates influence the extent and intensity of diagenetic processes in surficial intervals of organic-rich sediment column, leading to advanced mineralization of organic matter under suboxic conditions and to the related deposition of Fe-rich diagenetic carbonates (Coleman *et al.* 1979, Pisciotta and Mahoney 1981, Curtis 1987). This early diagenetic system seems to have dominated the base of the Agardhfjellet Formation in central Spitsbergen, and contributed to the formation of a well-developed cementstone band. Oxygen bottom water deficiency and accelerated sedimentation rates favour immediate development of sulphidic environment in organic-rich marine sediment, thus leading to preferential formation of iron sulphides instead of iron carbonates. Precipitation of carbonates becomes important in deeper diagenetic zones after significant reduction of

marine sulphate in pore waters (Curtis and Coleman 1986, Scotchman 1989). This early diagenetic system seems to have dominated the base of the Agardhfjellet Formation in the Bellsund area. Burial ankerite cementation and replacement took place in the two areas due primarily to thermally-induced decarboxylation and dissolution of biogenic calcite, and it was associated with advanced alteration of glauconite and other clay minerals and with dissolution of apatite.

## Conclusions

Petrographic, major element geochemical, and stable carbon and oxygen isotopic analyses of the Marhøgda Bed at Sassenfjorden and Van Keulenfjorden in Spitsbergen, Svalbard indicate that this lithostratigraphic unit is not a depositional limestone facies, but a diagenetic cementstone band originated at base of organic-rich sediment column of the Agardhfjellet Formation. Siderite and, to a lesser extent, ankerite are the most volumetrically important diagenetic carbonate minerals in the Bed. The abundance of Fe-rich diagenetic carbonates is typical of the Agardhfjellet Formation, and probably results from an abundance of reactive iron in organic-rich facies in Late Jurassic sedimentary basin in Svalbard.

Two episodes of carbonate diagenesis, including early precipitation of siderite and burial precipitation of ankerite, have contributed to the development of the Marhøgda Bed at Sassenfjorden. Early siderite precipitation in the Marhøgda Bed at Van Keulenfjorden was widely inhibited by pyrite formation, though burial precipitation of ankerite was of nearly equal importance. Extensive siderite precipitation at Sassenfjorden occurred at sedimentary temperatures in nearsurface suboxic zone in which microbial reduction of ferric iron compounds was the dominant diagenetic process. Burial precipitation of ankerite at the two studied locations occurred at temperatures of about 80–100°C in diagenetic environment overwhelmed by thermal decarboxylation processes. Compositional variations of ankerite between the studied locations reflect changing composition of pore waters in the Agardhfjellet Formation and the availability of iron- and manganese-containing mineral phases that escaped dissolution in surficial diagenetic zones. Burial formation of ankerite was associated with advanced alteration of glauconite and dissolution of apatite. Kaolinite precipitated as the major non-carbonate diagenetic cement.

Possible controls on the course of early diagenesis in the Marhøgda Bed embraced differences in bottom water oxygenation and in sedimentation rate during the deposition of basal sediments of the Agardhfjellet Formation. Formation of well-defined cementstone band at Sassenfjorden required development and maintenance of suboxic diagenetic zone close to the sediment/water interface, and was associated with elevated oxygenation of bottom water, suppressed sedimentation rates, and intense mineralization of organic matter. Oxygen bottom water deficiency and accelerated sedimentation rates at Van Keulenfjorden favoured imme-

diate development of anoxic sulphidic conditions in the sediment, which led to preferential formation of iron sulphides instead of iron carbonates, as well as to enhanced preservation of organic matter.

**Acknowledgements.** — The material analyzed in this paper was collected by KPK during the Polish Polar Expeditions to Spitsbergen in 1985 and 1986. The fieldwork was supported by Research Project No. CPBP 03.03.B5 of the Polish Academy of Sciences supervised by Professor Krzysztof Birkenmajer. The carbon and oxygen isotopic analysis was done at the Stable Isotope Laboratory of the Polish Academy of Sciences in Warszawa. The paper benefited from reviews by Associate Professor Paweł M. Leśniak and Dr Krzysztof Malkowski.

## References

- BÄCKSTROM S.A. and NAGY J. 1985. Depositional history and fauna of a Jurassic phosphorite conglomerate (the Brentskardhaugen Bed) in Spitsbergen. — *Norsk Polarinst. Skrifter* 183, 44 pp.
- BAUSCH W.M., BIRKENMAJER K., GRUNENBERG T., KRAJEWSKI K.P. and KUTYBA J. 1998. Clay-mineralogy of Jurassic marine shales in Spitsbergen: a possible evidence for climate cooling during Oxfordian. — *Pol. Acad. Sci. Bull., Earth Sci.* 46, 211–221.
- BECKER R.H. and CLAYTON R.N. 1976. Oxygen isotope study of a Precambrian banded iron-formation, Hamersley Range, Western Australia. — *Geochim. Cosmochim. Acta* 40, 1153–1165.
- BERNER R.A. 1981. A new geochemical classification of sedimentary environments. — *Jour. Sediment. Petrol.* 51, 359–365.
- BIRKENMAJER K. 1972. Megaripples and phosphorite pebbles in the Rhaeto-Liassic beds of Van Keulenfjorden, Spitsbergen. — *Norsk Polarinst. Årbok* 1970, 117–127.
- BIRKENMAJER K. 1975. Jurassic and Lower Cretaceous sedimentary formations of SW Torell Land, Spitsbergen. — *Studia Geol. Polon.* 44, 7–42.
- BIRKENMAJER K. 1979. Lower Cretaceous twin dolerite sills at Agardhbukta (east Spitsbergen) and the problem of thermal metamorphism of Mesozoic palynomorphs. — *Studia Geol. Polon.* 60, 57–63.
- BIRKENMAJER K. and PUGACZEWSKA H. 1975. Jurassic and Lower Cretaceous marine fauna of SW Torell Land, Spitsbergen. — *Studia Geol. Polon.* 44, 45–88.
- CANFIELD D.E. 1994. Factors influencing organic carbon preservation in marine sediments. — *Chem. Geol.* 114, 315–329.
- CLAYPOOL G.E. and KAPLAN I.R. 1974. The origin and distribution of methane in marine sediments. *In: I.R. Kaplan (ed.), Natural Gases in Marine Sediments.* Plenum, New York, pp. 99–139.
- COLEMAN M.L. 1985. Geochemistry of diagenetic non-silicate minerals: kinetic considerations. — *Phil. Trans. R. Soc London A315*, 39–56.
- COLEMAN M.L., CURTIS C.D. and IRWIN H. 1979. Burial rate: a key to source and reservoir potential. — *World Oil* 188, 93–92.
- CURTIS C.D. 1987. Inorganic geochemistry and petroleum exploration. *In: J. Brooks and D. Welte (eds), Advances in Petroleum Geochemistry, 2.* Academic Press, London, pp. 91–140.
- CURTIS C.D. and COLEMAN M.L. 1986. Controls on the precipitation of early diagenetic calcite, dolomite, and siderite concretions in complex depositional sequences. *In: D.L. Gautier et al. (eds), Roles of Organic Matter in Sediment Diagenesis.* SEPM Spec. Publ. 38, 23–33.
- DALLMANN W.K. (ed.) 1999. Lithostratigraphic Lexicon of Svalbard. Upper Palaeozoic to Quaternary Bedrock. Review and Recommendations for Nomenclature Use. *Norsk Polarinstutt, Tromsø*, 318p.

- DITCHFIELD P.W. 1997. High northern palaeolatitude. Jurassic–Cretaceous palaeotemperature variations: new data from Kong Karls Land, Svalbard. — *Palaeogeogr. Palaeoclimatol. Palaeoecol.* 130, 163–175.
- DRUMMOND S.E. and PALMER D.A. 1986. Thermal decarboxylation of acetate. Part II. Boundary conditions for the role of acetate in the primary migration of natural gas and the transportation of metals in hydrothermal systems. — *Geochim. Cosmochim. Acta* 50, 825–833.
- DYPVIK H. 1978. Origin of carbonate in marine shales of the Janusfjellet Formation, Svalbard. — *Norsk Polarinst. Årbok* 1977, 101–110.
- DYPVIK H. 1985. Jurassic and Cretaceous black shales of the Janusfjellet Formation, Svalbard, Norway. — *Sediment. Geol.* 41, 235–248.
- DYPVIK H., NAGY J., EIKELAND T.A., BACKER-OWE K. and JOHANSEN H. 1991a. Depositional conditions of the Bathonian to Hauterivian Janusfjellet Subgroup, Spitsbergen. — *Sediment. Geol.* 72, 55–78.
- DYPVIK H., NAGY J., EIKELAND T.A., BACKER-OWE K., ANDERSEN A., HAREMO P., BJÆRKE T., Johansen H. and Elverhri A. 1991b. The Janusfjellet Subgroup (Bathonian to Hauterivian) on central Spitsbergen: a revised lithostratigraphy. — *Polar Res.* 9, 21–43.
- FISHER R.S. and LAND L.S. 1986. Diagenetic history of Eocene Wilcox sandstones, South-Central Texas. — *Geochim. Cosmochim. Acta* 50, 551–561.
- FRITZ P. 1976. Oxygen and carbon isotopes in ore deposits in sedimentary rocks. In: K.H. Wolf (ed.), *Handbook of Strata-Bound and Stratiform Ore Deposits. I. Principles and General Studies. Vol. 2, Geochemical Studies.*
- GAUTIER D.L. 1985. Interpretation of early diagenesis in ancient marine sediments. In: D.L. Gautier, Y.K. Kharaka and R.C. Surdam (eds), *Relationship of Organic Matter and Mineral Diagenesis. SEPM Short Course Notes* 17, 6–78.
- GULBRANDSEN R.A. 1970. Relation of carbon dioxide content of apatite of the Phosphoria Formation to regional facies. — *U.S. Geol. Survey Prof. Paper* 700B, B9–B13.
- HARLAND W.B. 1997. *The Geology of Svalbard.* — *Geol. Soc. London Mem.* 17, 521p.
- HENDRY J.P., WILKINSON M., FALLICK A.E. and HASZELDINE R.S. 2000. Ankerite cementation in deeply buried Jurassic sandstone reservoirs of the central North Sea. — *Jour. Sediment Res.* 70, 227–239.
- HUGGETT J., DENNIS P. and GALE A. 2000. Geochemistry of early siderite cements from the Eocene succession of Whitecliff Bay, Hampshire Basin, U.K. — *Jour. Sediment. Res.* 70, 1107–1117.
- IRWIN H., CURTIS C. and COLEMAN M. 1977. Isotopic evidence for source of diagenetic carbonates formed during burial of organic-rich sediments. — *Nature* 269, 209–213.
- KHARAKA Y., LAW L.M., CAROTHERS W.W. and GOERLITZ D.F. 1986. Role of organic species dissolved in formation waters from sedimentary basins in mineral diagenesis. In: D.L. Gautier (ed.), *Roles of Organic Matter in Sediment Diagenesis.* — *SEPM Spec. Publ.* 38, 111–122.
- KOPIK J. and WIERZBOWSKI A. 1988. Ammonites and stratigraphy of the Bathonian and Callovian at Janusfjellet and Wimanfjellet, Sassenfjorden, Spitsbergen. — *Acta Palaeont. Polon.* 33, 145–168.
- KRAJEWSKI K.P. 1989. Organic geochemistry of a phosphorite to black shale transgressive succession: Wilhelmrya and Janusfjellet Formations (Rhaetian–Jurassic) in central Spitsbergen, Arctic Ocean. — *Chem. Geol.* 74, 249–263.
- KRAJEWSKI K.P. 1990. Phosphoritization in a starved shallow shelf environment: The Brentskardhaugen Bed (Toarcian–Bajocian) in Spitsbergen. — *Polish Polar Res.* 11, 331–334.
- KRAJEWSKI K.P. 1992a. Phosphorite-bearing sequence of the Wilhelmrya Formation in Van Keulenfjorden, Spitsbergen. — *Studia Geol. Polon.* 98, 171–199.
- KRAJEWSKI K.P. 1992b. Phosphorite-bearing sequence of the Wilhelmrya Formation at Hornsund and along western coast of Sörkapp Land, Spitsbergen. — *Studia Geol. Polon.* 98, 201–233.
- KRAJEWSKI K.P. 2001. Diagenetic recrystallization of apatite in phosphate nodules of the Brentskardhaugen Bed (Jurassic) in Spitsbergen. — *Bull. Pol. Acad. Sci, Earth Sci.* 49, 71–87.

- LAND L.S. 1985. The origin of massiv dolomite. — *Jour. Geol. Educ.* 33, 112–125.
- LEWAN M.D. and FISHER J.B. 1994. Organic acids from petroleum source rocks. *In*: E.D. Pittman and M.D. Lewan (eds), *Organic Acids in Geological Processes*. Springer-Verlag, Berlin, pp. 70–114.
- LONGSTAFFE F.J. 1983. Diagenesis, IV. Stable isotope studies of diagenesis in clastic rocks. — *Geosci. Can.* 10, 44–58.
- LUNDEGARD P.D. and KHARAKA Y.K. 1990. Geochemistry of organic acids in subsurface waters: field data, experimental data and models. *In*: D.C. Melchior and R.L. Basset (eds), *Chemical Modelling of Aqueous Systems. II*. Amer. Chem. Soc., Symp. Ser. 416, 169–189.
- LUNDEGARD P.D. and LAND L.S. 1986. Carbon dioxide and organic acids: their role in porosity enhancement and cementation, Paleogene of the Texas Gulf Coast. *In*: D.L. Gautier (ed.), *The Roles of Organic Matter in Diagenesis*. — *SEPM Spec. Publ.* 38, 129–146.
- MAHER H.D. Jr. 1989. A storm-related origin for the Jurassic Brentskardhaugen Bed of Spitsbergen, Norway. — *Polar Res.* 7, 67–77.
- MATSUMOTO R. and IJIMA A. 1981. Origin and diagenetic evolution of Ca-Mg-Fe carbonates in some coalfields of Japan. — *Sedimentology* 28, 239–259.
- MAYNARD J.B. 1982. Extension of Berner's "New geochemical classification of sedimentary environments" to ancient sediments. — *Jour. Sediment. Petrol.* 52, 1325–1331.
- MEANS J.L. and HUBBARD N. 1987. Short-chain aliphatic acid anions in deep subsurface brines: A review of their origin, occurrence, properties, and importance and new data on their distribution and geochemical implications in the Palo Duro Basin, Texas. — *Org. Geochem.* 11, 177–191.
- MØRK A., KNARUD R. and WORSLEY D. 1982. Depositional and diagenetic environments of the Triassic and Lower Jurassic succession of Svalbard. *In*: A.F. Embry and H.R. Balkwill (eds), *Arctic Geology and Geophysics*. — *Can. Soc. Petroleum Geologists Mem.* 8, 371–398.
- MØRK A., DALLMANN W.K., DYPVIK H., JOHANNESSEN E.P., LARSEN G.B., NAGY J., NØTTVEDT A., OLAUSSEN S., PČELINA T.M. and WORSLEY D. 1999. Mesozoic lithostratigraphy. *In*: W.K. Dallmann (ed.), *Lithostratigraphic Lexicon of Svalbard. Review and Recommendations for Nomenclature Use. Upper Palaeozoic to Quaternary Bedrock*. Norsk Polarinstittutt, Tromsø, p. 127–214.
- MORTIMER R.J.G. and COLEMAN M.L. 1997. Microbial influence on the oxygen isotopic composition of diagenetic siderite. *Geochim.* — *Cosmochim. Acta* 61, 1705–1711.
- MOZLEY P.S. 1989a. Relation between depositional environment and the elemental composition of early diagenetic siderite. — *Geology* 17, 704–706.
- MOZLEY P.S. 1989b. Complex compositional zonation in concretionary siderite: implications for geochemical studies. — *Jour. Sediment. Petrol.* 59, 815–818.
- MOZLEY P.S. and CAROTHERS W.W. 1992. Elemental and isotopic composition of siderite in the Kuparuk Formation, Alaska: effect of microbial activity and water/sediment interaction on early pore-water chemistry. — *Jour. Sediment. Petrol.* 62, 681–692.
- MOZLEY P.S. and BURNS S.J. 1993. Oxygen and carbon isotopic composition of marine carbonate concretions: an overview. — *Jour. Sediment. Petrol.* 63, 73–83.
- PČELINA T.M. 1980. New data on the Uppermost Triassic–Lowermost Jurassic strata in Svalbard archipelago. *In*: D.V. Semevski (ed.), *Geology of the Sedimentary Cover of Svalbard*. Izd. Nida, Leningrad, pp. 43–60 (in Russian).
- PISCIOTTO K.A. and MAHONEY J.J. 1981. Isotopic survey of diagenetic carbonates, DSDP Leg 63. Initial Report of the Deep Sea Drilling Project 63, 595–609.
- SCHUFFERT J.D., KASTNER M., EMANUELE G. and JAHNKE R.A. 1990. Carbonate-ion substitution in francolite: A new equation. — *Geochim. Cosmochim. Acta* 54, 2323–2328.
- SCOTCHMAN I.C. 1989. Diagenesis of the Kimmeridge Clay Formation, onshore UK. — *Jour. Geol. Soc. London* 146, 285–303.

- STEEL R.J. and WORSLEY D. 1984. Svalbard's post-Caledonian strata – An atlas of sedimentational patterns and palaeogeographic evolution. *In: A.M. Spencer et al. (eds), Petroleum Geology of the North European Margin*. Nor. Pet. Soc., Graham and Trotman, London, p.109–135.
- ROSENBAUM J. and SHEPPARD S.M. 1986. An isotopic study of siderites, dolomites and ankerites at high temperatures. — *Geochim. Cosmochim. Acta* 50, 1147–1150.
- RÓŻYCKI S.Z. 1959. Geology of the north-western part of Torell Land, Vestspitsbergen. — *Studia Geol. Polon.* 2, 7–98.
- THORNBURG T.M. and SUSS E. 1990. Carbonate cementation of granular and fracture porosity: implications for the Cenozoic hydrologic development of the Peru continental margin. — *Proceedings of the Ocean Drilling Program, Sci. Results* 112, 95–109.
- WHITICAR M.J. 1999. Carbon and hydrogen isotope systematics of bacterial formation and oxidation of methane. — *Chem. Geol.* 161, 291–314.
- WHITICAR M.J., FABER E. and SCHOELL M. 1986. Biogenic methane formation in marine and fresh-water environments: CO<sub>2</sub> reduction vs. acetate fermentation – Isotopic evidence. — *Geochim. Cosmochim. Acta* 50, 693–709.
- WIERZBOWSKI A., BIERNAT G. and KULICKI C. 1981a. Stratigraphic position and remarks on sedimentation of the Brentskardhaugen Bed (Spitsbergen). — *Pol. Geogr. Soc., Polar Symp.*, 8: 181–191.
- WIERZBOWSKI A., KULICKI C. and PUGACZEWSKA H. 1981b. Fauna and stratigraphy of the Uppermost Triassic and the Toarcian and Aalenian deposits in Sassenfjorden, Spitsbergen. — *Acta Palaeont. Polon.* 26, 195–237.

Received February 23, 2001

Accepted April 23, 2001

## Streszczenie

Warstwa z Marhøgda jest formalną jednostką litostratygraficzną występującą lokalnie u podstawy jurajskiej formacji z Agardhfjellet na Spitsbergenie, archipelag Svalbard (fig. 1–3). Warstwa ta była interpretowana jako oolitowa facja wapienna osadzona w początkowym stadium górnourajskiej fazy transgresywnej na Svalbardzie. Dokładne badania petrograficzne (fig. 4–12), geochemiczne (tab. 1–5; fig. 13–17) oraz analiza izotopów stabilnych węgla i tlenu (tab. 6; fig. 18–22) wskazują, iż warstwa z Marhøgda nie zawiera depozycyjnych węglanów, a występujący w niej syderyt i ankeryt jest wyłącznie pochodzenia diagenetycznego. Koncentracja minerałów węglanowych u podstawy formacji z Agardhfjellet była wynikiem dwóch epizodów cementacji osadu związanych z etapami diagenetycznej degradacji osadowej substancji organicznej (fig. 23): 1) wczesnodiagenetycznej cementacji syderitem w przypowierzchniowej strefie suboksydacyjnej zdominowanej przez mikrobiologiczne utlenianie substancji organicznej i redukcję tlenków żelaza; 2) późnodiagenetycznej cementacji ankerytem w warunkach głębokiego pogrzebienia i podwyższonej temperatury (80–100°C) w środowisku zdominowanym przez abiotyczne procesy dekarboksylacji kerogenu.